KfK 3454
Januar 1983

MEDUSA-KA: A One-Dimensional Computer Code for Inertial Confinement Fusion Target Design

N. A. Tahir, K. A. Long
Institut für Neutronenphysik und Reaktortechnik

Kernforschungszentrum Karlsruhe

KERNFORSCHUNGSZENTRUM KARLSRUHE

Institut für Neutronenphysik und Reaktortechnik

KfK 3454

MEDUSA-KA: A One-Dimensional Computer Code for Inertial Confinement Fusion Target Design

N.A. Tahir and K.A. Long

Kernforschungszentrum Karlsruhe GmbH, Karlsruhe

Kernforschungszentrum Karlsruhe GmbH
ISSN 0303-4003

Abstract

In this report we describe an updated version of the one-dimensional, two-temperature, Lagrangian computer code MEDUSA, which was developed at the Culham Laboratory, England. We present an extensive review of the standard version of this code together with the modifications made to this code at the Glasgow University and the Rutherford Laboratory, England, in order to make it suitable to simulate laser-compression experiments performed at the Rutherford Laboratory. We also describe the modifications made to this code at the Institut für Neutronenphysik und Reaktortechnik in order to transform this code to an ion-beam fusion code. This updated version of the MEDUSA code, MEDUSA-KA has been used to design heavy ion-beam targets for the HIBALL reactor study. A summary of these calculations is included in this report. This code can be used to design other types of ICF targets including laser-fusion targets and light ion-beam targets.

MEDUSA-KA: Ein eindimensionales Rechenprogramm für den Entwurf von Trägheitseinschlußfusionstargets

Zusammenfassung

Im vorliegenden Bericht wird eine verbesserte Version des Lagrangeschen eindimensionalen, Zwei-Temperatur-Rechenprogramms MEDUSA beschrieben, das im Culham Laboratory, England, entwickelt wurde. Es wird ein ausführlicher Überblick gegeben über die Standardversion dieses Programms und die Änderungen, die in der Universität Glasgow und im Rutherford Laboratory, England, vorgenommen wurden, um das Programm für die Simulierung der im Rutherford Laboratory durchgeführten Laser-Kompressionsexperimente geeignet zu machen. Ebenso beschrieben werden die Änderungen, die im Institut für Neutronenphysik und Reaktortechnik an diesem Programm vorgenommen wurden, um es in ein Rechenprogramm für Ionenstrahl-Fusion umzuwandeln. Diese verbesserte Version des Programms MEDUSA, MEDUSA-KA, wird benutzt zur Auslegung von Schwerionenstrahltargets für die HIBALL-Reaktorstudie. Eine Zusammenfassung der Berechnungen ist im vorliegenden Bericht enthalten. Das Rechenprogramm kann auch zur Auslegung anderer Arten von Targets für die Trägheitsfusion eingesetzt werden, einschließlich Laserfusionstargets und Leichtionenstrahltargets.

Table of Contents

		page
1.	Introduction	1
2.	Review of Standard Version of MEDUSA	3
	2.1 Physical and Mathematical Model	3
	System of equations	4
	Energy equations	5
	Thermal conduction	6
	Energy exchange	7
	Bremsstrahlung losses	8
	Input power absorption	8
	Thermonuclear energy absorption	9
	Viscous shock heating	10
	Equation of motion	11
	2.2 Geometry Options and Boundary Conditions	12
	2.3 Numerical Solution of the Problem	14
	Description of mesh and time level scheme	14
	Finite difference scheme	16
	Time step control	23
	Calculation of energies	24
	2.4 Limitations of the original version of MEDUSA	27
3.	Updated Version of MEDUSA at KfK (MEDUSA-KA)	29
	3.1 MEDUSA at Glasgow University	29
	Target design	29
	Atomic physics	29
	Radiation transport	31
	3.2 MEDUSA at Rutherford Laboratory	32
	Target design	33
	Equation of state	33
	Atomic physics	33
	Hot electrons	33
	Ion-beam energy deposition	34

Table of Contents (cont.)

		page
3.3	MEDUSA at INR (Karlsruhe)	34
	Target initial conditions	40
	Atomic physics in MEDUSA-KA	43
	Equation of state	43
	Energy deposition	53
	Modifications in the numerics of the code to allow for hollow shells	57
3.4	Future Developments	58
4.	Instructions to Users	60
4.1	Input Specification and Output Control	60
	Input specification	60
	List of equivalences	65
	Use of array LASER1(301)	66
	Use of array PIQ(301)	67
	Output control and numerical control	68
	Error messages	69
4.2	List of Subroutines	70
4.3	List of Common Blocks	72
4.4	List of Common Variables	73
5.	Extended Test Problem	83
5.1	Input Data	83
5.2	Discussion of Results	85
5.3	Selected Output from MEDUSA-KA Test Run	88
Acknowledgements		93
References		94

1. Introduction

The original version of MEDUSA /1/ was written in 1973 in order to study the feasibility of laser-fusion as a method for generating thermonuclear power proposed in references /2,3/. This code can be used to study one-dimensional hydrodynamic and thermodynamic response of an inertial confinement fusion (ICF) target irradiated by an intense laser beam. This code can handle a solid micro-sphere, a cylindrical target and a plane target. The first and the second type of geometries are used to study implosion problems while the plane targets are used to study laser-plasma interaction problems. The physical model of this code treats the plasma as a charge neutral mixture of electrons and ions of one or more species with a fixed degree of ionization. This model does not allow for ionization or recombination. The thermodynamics of this code treats the ions and the electrons as two independent sub-systems with individual thermodynamic variables whereas the hydrodynamics regards the plasma as a single fluid having a hydrodynamic velocity u. The electrons and the ions are coupled together via this common hydrodynamic velocity and an electron-ion energy exchange term. The ions are always regarded as a classical system while the electrons can either be classical or degenerate depending on the plasma density and temperature. The input laser energy is absorbed in the plasma at sub-critical densities via inverse Bremsstrahlung and the rest of the energy is dumped in the critical density cell. This energy is transported from the absorption region to the ablation front via ion and electron thermal conduction.

A detailed review of this computer code /1/ which includes the physical and mathematical model, a description of the mesh and time-level scheme, different boundary conditions and options available, numerical techniques employed to solve the problem and the limitations of this model are given in Sec. 2 of this report.

Since the standard version of the code was published, extensive modifications were done to the code at the University of Glasgow /4,5,6,7,8/ and the Central Laser Facility, Rutherford Laboratory /9,10,11/. These modifications were done in order to allow for various important geometrical options and physical phenomena which were outside the scope of the standard

version of the code and were essential to simulate laser-compression experiments performed at the Rutherford Laboratory.

There has been a growing interest in the Federal Republic of Germany in the employment of heavy and light ion beams as a driver for the ICF reactor systems. Recently, a reactor study known as "HIBALL" /12/ which is a conceptual study of a heavy ion beam driven ICF reactor was carried out by various research groups in the Federal Republic of Germany and the University of Wisconsin. The MEDUSA code was used to design the ion-beam targets for this reactor study /13,14,15,16,17,18,19/. In Sec. 3 we describe the modifications made to MEDUSA in order to transform it to an ion-beam fusion code MEDUSA-KA at the Institut für Neutronenphysik und Reaktortechnik, Karlsruhe. In Sec. 4 we provide the necessary information for users to run this code and in Sec. 5 we present a standard test problem.

2. A Review of the Standard Version of MEDUSA.

2.1 Physical and Mathematical Model

The physical model used in this code assumes that the target is a charge neutral mixture of electrons and ions of various species with a fixed degree of ionization. The electrons and the ions are treated as two independent thermodynamic sub-systems with individual thermodynamic variables. The quantities with subscript e refer to the electrons whereas those with i are the corresponding quantities for the ions. These two sub-systems, however, have the same hydrodynamic velocity and are also coupled with each other via an electron-ion energy exchange term. The standard version of MEDUSA /1/ considers 8 species of ions, namely, hydrogen (H), deuterium (D), tritium (T), helium3 (He^3), helium4 (He^4), neutral atoms (N) with mass number M_N, an arbitrary ion (X) with mass number M_x and charge number Z_x and neutrons (n). All the ionic species and the neutral atoms except the neutrons are carried along with the hydrodynamics. The neutrons, on the other hand, are allowed to escape freely from the plasma, thereby leading to a loss of mass and a change in momentum. The instantaneous local chemical composition of the plasma is described in the code by a set of fractions f_k such that

$$n_k = f_k \, n_i \tag{2.1}$$

is the number density of ions of species k. This fraction can only change when the target undergoes nuclear fusion and is adjusted at every time step to maintain the normalization

$$\sum_k f_k = 1 \tag{2.2}$$

A similar fraction f_n is used for the neutrons which have been produced by each element (Lagrangian cell) of the target, but this is not included in equation (2.2). In (2.1) n_i is the total number density of the ions.

System of equations.

The average mass and charge number associated with each ion are respectively given by

$$M = \sum_k f_k M_k$$

$$z = \sum_k f_k z_k \qquad (2.3)$$

where M_k and z_k denote mass number and charge number of individual species. The electron number density is then given by

$$n_e = z\, n_i \qquad m^{-3} \qquad (2.4)$$

The physical mass density can be written as

$$\rho = n_i M m_H = \frac{1}{v} \qquad kg/m^3 \qquad (2.5)$$

where m_H is the proton mass and v is the specific volume. The electron mass, the neutron and proton mass difference and all mass defects are neglected in this model.

The two sub-systems have separate equations of state (EOS) of the form

$$U = U(\rho, T) \qquad J/kg$$

$$P = P(\rho, T) \qquad J/m^3 \qquad (2.6)$$

which denote internal energy and pressure respectively; T is the temperature. The EOS in general may not be the same for the two sub-systems. This is due to the fact that the ions are always treated as a classical sub-system in which case equations (2.6) reduce to

$$U_i = \frac{3}{2} \frac{KT_i}{m_H M} \qquad J/kg$$

$$\text{and} \qquad P_i = n_i KT_i \qquad J/m^3 \qquad (2.7)$$

where K is the Boltzmann's constant and the quantities with subscript i are the quantities associated with the ions. The electrons, on the other hand, can either be classical or fully or partially degenerate, depending on the density and temperature of the region. The degree of degeneracy of the electrons is checked by a parameter

$$\xi = T_e/T_F \tag{2.8}$$

where T_F is the Fermi temperature given by

$$KT_F = \frac{h^2}{8m_e}\left(\frac{3}{\pi}\right)^{2/3}\left(\frac{z}{Mm_H}\right)^{2/3}\rho^{2/3} \quad \text{J} \tag{2.9}$$

In the above equation h is Planck's constant and m_e is the electron mass. If ξ is $\geq \xi_{max}$ then the electrons are non-degenerate, if $\xi_{min} \leq \xi < \xi_{max}$ the electrons are partially degenerate and if $\xi < \xi_{min}$, the electrons are fully degenerate. Typically, in MEDUSA, $\xi_{min} = 0.38$ and $\xi_{max} = 1$. In case electrons are non-degenerate, their internal energy U_e and pressure P_e have similar expressions as for the ions but with n_i and T_i replaced by n_e and T_e respectively. In case when the electrons are degenerate, more complicated expressions are used to evaluate the thermodynamic quantities for the electrons, and will be discussed in Chapter 3.

Energy Equations:

$$\text{Electrons} : (C_v)_e \frac{dT_e}{dt} + (B_T)_e \frac{d\rho}{dt} + P_e \frac{dv}{dt} = S_e \quad \text{W/kg} \tag{2.10}$$

$$\text{Ions} : (C_v)_i \frac{dT_i}{dt} + P_i \frac{dv}{dt} = S_i \quad \text{W/kg} \tag{2.11}$$

In the above equations

$$C_v = \left(\frac{\partial U}{\partial T}\right)_\rho$$

is the specific heat and

$$B_T = \left(\frac{\partial U}{\partial \rho}\right)_T$$

is the compressibility. We note that since the ions are always considered as a classical system, the ion compressibility

$$\left(\frac{\partial U_i}{\partial \rho}\right)_{T_i} \equiv 0$$

The source terms S are given by

$$S_e = H_e + K_{ie} + Y_e + J + X \qquad \text{W/kg} \qquad (2.12)$$

$$S_i = H_e - K_{ie} + Y_i + Q \qquad \text{W/kg} \qquad (2.13)$$

In the above equations, H denotes thermal conduction rate, K_{ie} is the electron-ion energy exchange rate, Y is the rate of energy deposited by the α-particles produced in the nuclear reactions, J is the Bremsstrahlung loss rate, Q is the viscous shock heating rate and X is the rate of energy absorbed from the driver. Expressions for these quantities are discussed below.

Thermal conduction:

$$H = \frac{1}{\rho} \nabla \cdot \kappa \nabla T \qquad (2.14)$$

where κ is the thermal conductivity

$$\kappa_i = 4.3\times10^{-12} T_i^{5/2} (\log\Lambda)^{-1} \overline{M^{-1/2} z^{-2}} \; \overline{(z^2)}^{-1} \qquad \text{W/mK} \qquad (2.15)$$

and $$\kappa_e = 1.83\times10^{-10} T_e^{5/2} (\log\Lambda)^{-1} \; z\overline{(z^2)}^{-1} \qquad \text{W/mK} \qquad (2.16)$$

Also $$\Lambda = 1.24 \; 10^7 T_e^{3/2} n_e^{-1/2} / z \qquad (2.17)$$

It is seen from the above equation that for the same temperature, the electron thermal conductivity is much greater than the ion thermal conductivity. It is also to be noted that the diffusion flux

$$F_e = \kappa_e \nabla T_e \qquad \text{W/m}^2 \qquad (2.18)$$

becomes unphysically large for very sharp temperature gradients, which merely signifies the inapplicability of the diffusion approximation. In order to restrict the thermal flux, an upper limit known as "the free streaming limit", is imposed on the thermal flux as following

$$\frac{1}{F_e'} = \frac{1}{F_e} + \frac{1}{(F_e)_{max}} \tag{2.19}$$

where the free streaming limit

$$(F_e)_{max} = a \cdot \frac{1}{4} \cdot n_e \overline{v_e} K T_e \tag{2.20}$$

a is an adjustable parameter known as the "Flux Limiter". For a = 1, $(F_e)_{max}$ corresponds to the case when all the electrons are moving in the same direction. Substituting F_e and $(F_e)_{max}$ from (2.18) and (2.20) respectively in (2.19) we get a modified expression for κ_e as

$$\kappa_e' = \kappa_e \left(1 + a \frac{\lambda_e}{T_e}\left|\frac{dT_e}{dx}\right|\right)^{-1} \tag{2.21}$$

where $$\lambda_e = 5.7\times10^9 \; T_e^2/(n_i \overline{z^2} \log\Lambda) \quad m \tag{2.22}$$

and is the electron mean free path (mfp).

Energy Exchange:

It is considered that the ions and the electrons exchange energy as a function of their local temperature difference as described below

$$K_{ie} = (C_v)_i \cdot \omega_{ie} \cdot (T_i - T_e) \qquad W/kg \tag{2.23}$$

where $$\omega_{ie} = \frac{M^{-1} \overline{z^2} \; e^4 \; n_i \; \log\Lambda \; m_e^{1/2}}{32\sqrt{2\pi} \; \varepsilon_o^2 \; m_H} (KT_e)^{-3/2} \quad s^{-1} \tag{2.24}$$

and is the electron-ion collision frequency /20/.

Bremsstrahlung Losses:

For a Maxwellian gas one can write /20/

$$J = \frac{-\overline{z^2}\, e^6\, n_e\, \overline{v_e}}{24\pi\varepsilon_o^3\, c^3\, m_e\, m_H\, M \cdot h} \tag{2.25}$$

where the symbols have their usual meaning. The above expression can be reduced to

$$J = -\, 8.5\times10^{-14}\, n_e\, T_e^{1/2}\, \overline{z^2}\, M^{-1} \tag{2.26}$$

Since Bremsstrahlung is a loss from the plasma, it is evaluated as a negative quantity. In case when the gas is Fermi-degenerate, one uses

$$J = -\, 8.5\times10^{-14}\, n_e\, \delta T_e^{1/2}\, \overline{z^2}\, M^{-1} \quad W/kg \tag{2.27}$$

where
$$\delta T_e = T_e - \left(\frac{n_e}{n_e^o}\right)^{\gamma_e - 1} T_e^o \tag{2.28}$$

In the above equation γ_e is the specific heat ratio for the electrons, n_e^o is the initial electron number density and T_e^o is the initial electron temperature which yields the same pressure as the Fermi pressure of a fully degenerate gas. Use of equation (2.27) in case of a degenerate electron gas prevents unphysical cooling of the electrons below Fermi minimum energy.

Input Power Absorption:

The standard version of MEDUSA is a laser-fusion code and it only allows for laser-energy absorption. At sub-critical densities the input energy is absorbed by inverse Bremsstrahlung while the rest of the input energy is dumped in the critical density cell, as discussed below.

The critical mass density can be written as

$$\rho_c = \frac{\varepsilon_o\, M\, m_H\, m_e}{ze^2}\, \omega_L^2 \quad kg/m^3 \tag{2.29}$$

where ω_L is the laser frequency.

The inverse Bremsstrahlung absorption coefficient is given by /21/

$$\alpha = 13.51\lambda^{-2}\beta^2(1-\beta)^{-1/2}T_e^{-3/2}(5.05+\log\Lambda\cdot T_e)\bar{z} \quad m^{-1} \tag{2.30}$$

where

$$\beta = \frac{\rho}{\rho_c} < 1$$

and λ is the wave length of the laser light. The laser power at a point r in the plasma at a time t can be written as

$$P_L(r,t) = e^{-\alpha(R_o-r)}P_L(R_o,t) \tag{2.31}$$

where $P_L(R_o,t)$ is the power incident on the target surface. The remaining power $P_L(r_c,t)$ is dumped in the cell with critical density.

Thermonuclear Energy Absorption:

MEDUSA considers in a D-T plasma the following four reactions

$$D + T = H_e^4(3.6MeV) + n(14.1MeV)$$
$$D + D = T(1.0MeV) + H(3.0MeV)$$
$$D + D = H_e^3(0.8MeV) + n(2.45MeV)$$
$$D + H_e^3 = H_e^4(3.6MeV) + H(14.7MeV)$$

The D-T reaction rate is given by

$$R_{DT} = (\sigma v)_{DT} f_D f_T n_i^2 \quad m^{-3}s^{-1} \tag{2.32}$$

with similar expressions for D-D and D-H_e^3.

Where $(\sigma v)_{DT}$ is a function of T_i and is given by /22/

$$(\sigma v)_{DT} = 3.68\times10^{-18}\cdot T_i^{-2/3}\cdot\exp(-19.94\cdot T_i^{-1/3}) \tag{2.33}$$

The cross sections for the other processes are given below:

$$(\sigma v)_{DD} = 2.33\times10^{-20}\cdot T_i^{-2/3}\cdot\exp(-19.94\cdot T_i^{-1/3}) \tag{2.34}$$

$$(\sigma v)_{DHe^3} = 10^{-23} \qquad T_i \geq 50 \text{ KeV} \tag{2.35}$$

In the above equations T_i is in KeV.

We note that in MEDUSA, the reaction cross sections are kept constant for values of T_i>35KeV. The reduction in the cross sections at higher temperatures is not considered.

The neutrons produced in the nuclear reactions escape freely while the charged particles including, H, T, He^3 and He^4 deposit their energy to the ions and the electrons locally in ratios which we write for D-T reactions as P_{DT} and $1-P_{DT}$ respectively. P_{DT} is a function of T_e /23/ given by:

$$P_{DT} = T_e/(T_e+3.71\times10^8) \tag{2.36}$$

Also expressions for P_{DD} and P_{DHe^3} are given by

$$P_{DD} = T_e/(T_e+1.2\times10^9) \tag{2.37}$$

$$P_{DHe^3} = T_e/(T_e+2\times10^9) \tag{2.38}$$

If E_{DT}, E_{DD} and E_{DHe^3} denote energies of charged reaction products produced in the corresponding reactions, then

$$Y_i = P_{DD}E_{DD}R_{DD} + P_{DT}E_{DT}R_{DT} + P_{DHe^3}E_{DHe^3}R_{DHe^3} \quad W/kg \tag{2.39}$$

with a similar expression for Y_e with P_{DT} etc. replaced by $1-P_{DT}$.

Viscous Shock Heating:

The viscous shock heating rate

$$Q = - q \frac{dv}{dt} \tag{2.40}$$

where q is the viscous pressure and is a function of ρ and hydrodynamic velocity u and will be treated in section 2.3.

Equation of Motion:

The motion of the plasma is handled by Navier-Stoke's equation

$$\rho \frac{du}{dt} = - \nabla P \tag{2.41}$$

where P is the total pressure including hydrodynamic as well as viscous pressure.

Also $$u(r,t) = \frac{dr}{dt} \tag{2.42}$$

2.2 Geometry Options and Boundary Conditions

Geometry.

MEDUSA can treat plane, cylindrical and spherical geometry depending on the choice of a parameter g which can be set in the input.

- g = 1 corresponds to a slab of unit cross section
- g = 2 represents a section of a cylinder of unit height and one radian in angle
- g = 3 represents a section of a sphere of one steradian solid angle.

Only the co-ordinate r is used in each case, the cross sections being required only for normalization purposes.

The option g = 1 is used to simulate laser (ion-beam) and plane target experiments while g = 2 can treat the liner implosions. Finally g = 3 can handle implosion (compression, ignition, burn and disassembly) of spherical ICF targets.

Boundary Conditions.

In order to make the specification of the problem complete and to solve the set of thermodynamic and hydrodynamic equations described in Section 2.1, one needs to specify the boundary conditions at the inner as well as the outer boundary of the target.

For the inner boundary, MEDUSA assumes $u(r=0) \equiv 0$ and zero thermal flux. For the outer moving boundary at $r = R_o$ (R_{N+1} in Fig. 2) one can choose either of the following four conditions depending on the type of the problem one considers.

(a) $P(R_o) = 0$, zero thermal flux

(b) $u(R_o) = 0$, $T_i(R_o) = T_i(t)$; $T_e(R_o) = T_e(t)$

(c) $P(R_o) = P(t)$, zero thermal flux

(d) $u(R_o) = u(t)$, zero thermal flux (2.43)

Case a is used to study problems involving laser (ion) energy absorption, case b is used to study simplified thermal conduction problems and cases c and d are used to study simplified hydrodynamic problems.

2.3 Numerical Solution of the Problem

The set of equations in MEDUSA is solved numerically and in this sub-section we discuss the details of these numerical methods.

Description of MESH and Time Level Scheme.

The target radius is replaced by a Lagrangian mesh shown in Fig. 1 which is divided into N cells of equal width at time, t = 0. The cell centres are labelled with ℓ while the cell boundaries are labelled with j. The inner boundary, $r = R_1 = 0$ remains fixed while the outer boundary of the first cell, R_2 together with R_3 .... R_{N+1} are free to move during the implosion and expansion phases. When the cell gets compressed the density increases while the cell mass remains constant unless nuclear reactions take place. The co-ordinates R and the velocities u of each cell are evaluated at the cell boundaries while the density ρ and the temperatures T_e and T_i are evaluated at the cell centres.

A 5-level time scheme is used in MEDUSA to advance the various quantities in time as shown in Fig. 2. These time levels are labelled by n-1, n-1/2, n, n+1/2 and n+1 respectively. A quantity with a superscript n means the value of that quantity at time level n.

Known quantities

R_j, ρ_ℓ, T_ℓ, f_K	at n-1
u_j	at n-1/2
R_j, ρ_ℓ	at n

where T stands for both T_e and T_i. Using the time integration scheme described in the next sub-section the above quantities are advanced in time as indicated below

T_ℓ, f_K	at time level n
u_j	at time level n+1/2
R_j, ρ_ℓ	at time level n+1

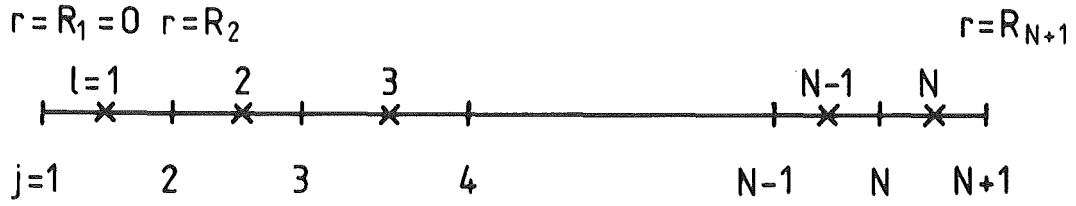

Figure 1. The arrangement of the mesh

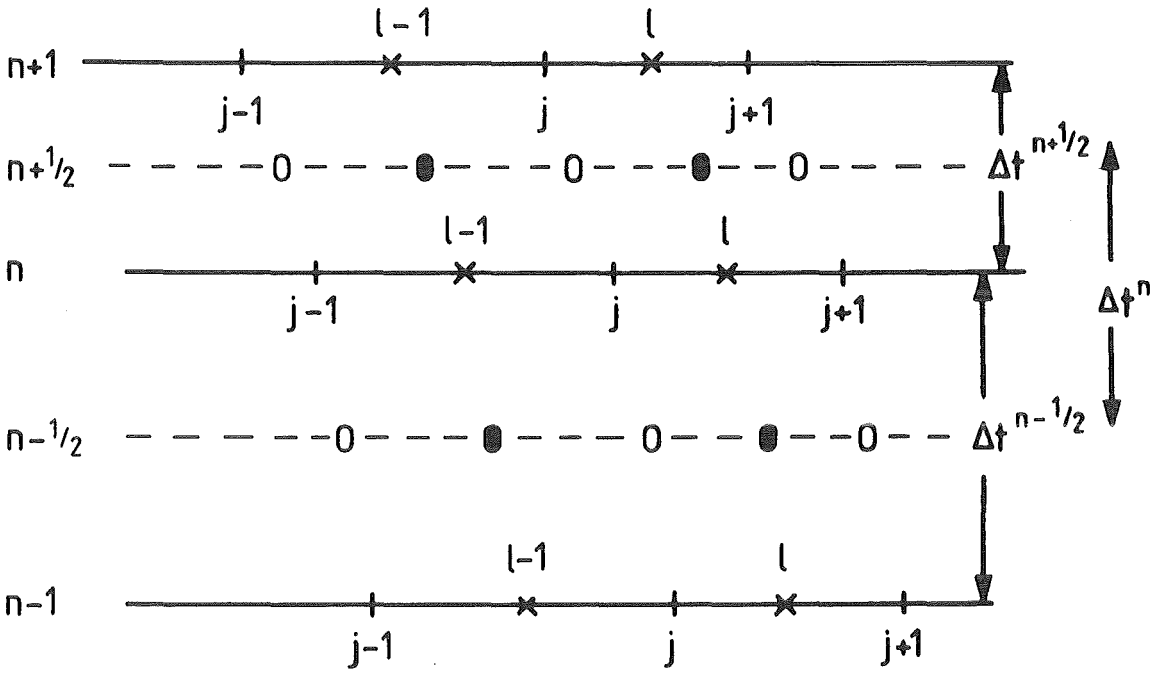

1 ~ R 0 ~ u

X ~ p , T_i , T_e ● ~ q

Figure 2. The 5 time levels indicating how the basic quantities are advanced

Finite Difference Scheme.

The two energy equations for the electrons and the ions are solved for their corresponding temperatures using Cranck-Nicolson's time centred scheme and Gauss's elimination method.

One can write for electrons as well as ions

$$(C_v)_\ell^{n-1/2} \frac{T_\ell^n - T_\ell^{n-1}}{\Delta t^{n-1/2}} + (B_T)_\ell^{n-1/2} \frac{\rho_\ell^n - \rho_\ell^{n-1}}{\Delta t^{n-1/2}}$$

$$+ P_\ell^{n-1/2} \frac{V_\ell^n - V_\ell^{n-1}}{\Delta t^{n-1/2}} = S_\ell^{n-1/2} \qquad (2.44)$$

For simplicity we omit the subscripts i or e. For the electrons the source term is given by (2.12) while for the ions one should replace S_e by (2.13). This leads to

$$[S_e]_\ell^{n-1/2} = [H_e]_\ell^{n-1/2} + [K_{ie}]_\ell^{n-1/2} + [Y_e]_\ell^{n-1/2} + [J]_\ell^{n-1/2}$$

$$+ [X_\ell]^{n-1/2} \qquad (2.45)$$

and $$[S_i]_\ell^{n-1/2} = [H_i]_\ell^{n-1/2} - [K_{ie}]_\ell^{n-1/2} + [Y_i]_\ell^{n-1/2} + [Q]_\ell^{n-1/2} \qquad (2.46)$$

In order to solve equation (2.44) for the temperature, T_ℓ^n, one needs to feed in all the coefficients on the L.H.S. and the source terms on the R.H.S. at appropriate time levels. All the quantities except $K_{ie}^{n-1/2}$ are evaluated at time level n-1/2 by simple averaging of the type

$$X_\ell^{n-1/2} = \frac{1}{2}\left[X_\ell^n + X_\ell^{n-1}\right] \qquad (2.47)$$

K_{ie} however requires special treatment to allow for large equipartition rates, as explained below.

Energy Exchange Rate:

Special care must be taken in choice of the time step when studying a system with widely disparate time scales even if one is employing implicit numerical schemes. In such a case the time step should be restricted according to the shortest time scale, otherwise one runs into trouble. This can be understood better by studying the following problem.

Consider the differential equation

$$\frac{\partial f}{\partial t} = - \omega f \tag{2.48}$$

where f may be a fraction of some radioactive material which decays on a time scale $\tau \sim \frac{1}{\omega}$.

Analytic solution to (2.48) is

$$f = f_o \, e^{-\omega t} \tag{2.49}$$

where $f_o \equiv f(t=0)$.

The numerical solution to equation (2.48) can be written as

$$\frac{f^{n+1} - f^n}{\Delta t} = - \omega \left[\theta f^{n+1} + (1-\theta) f^n \right] \tag{2.50}$$

where θ determines the degree of implicitness. Eq. (2.50) can be rewritten as

$$f^{n+1} = f^n \, \frac{1-\Delta t \cdot \omega \cdot (1-\theta)}{1+\Delta t \cdot \omega \cdot \theta} \tag{2.51}$$

It is seen that if ω is very large, then f^{n+1} can become negative unless Δt is chosen to be sufficiently small. Also it is seen from Fig. 3 that if we like to evaluate $f^{n+1/2}$ taking the average of f^{n+1} and f^n, it will be a very bad approximation and could introduce significant error. This problem can be solved if we fit the analytic solution to the numerical solution as shown below

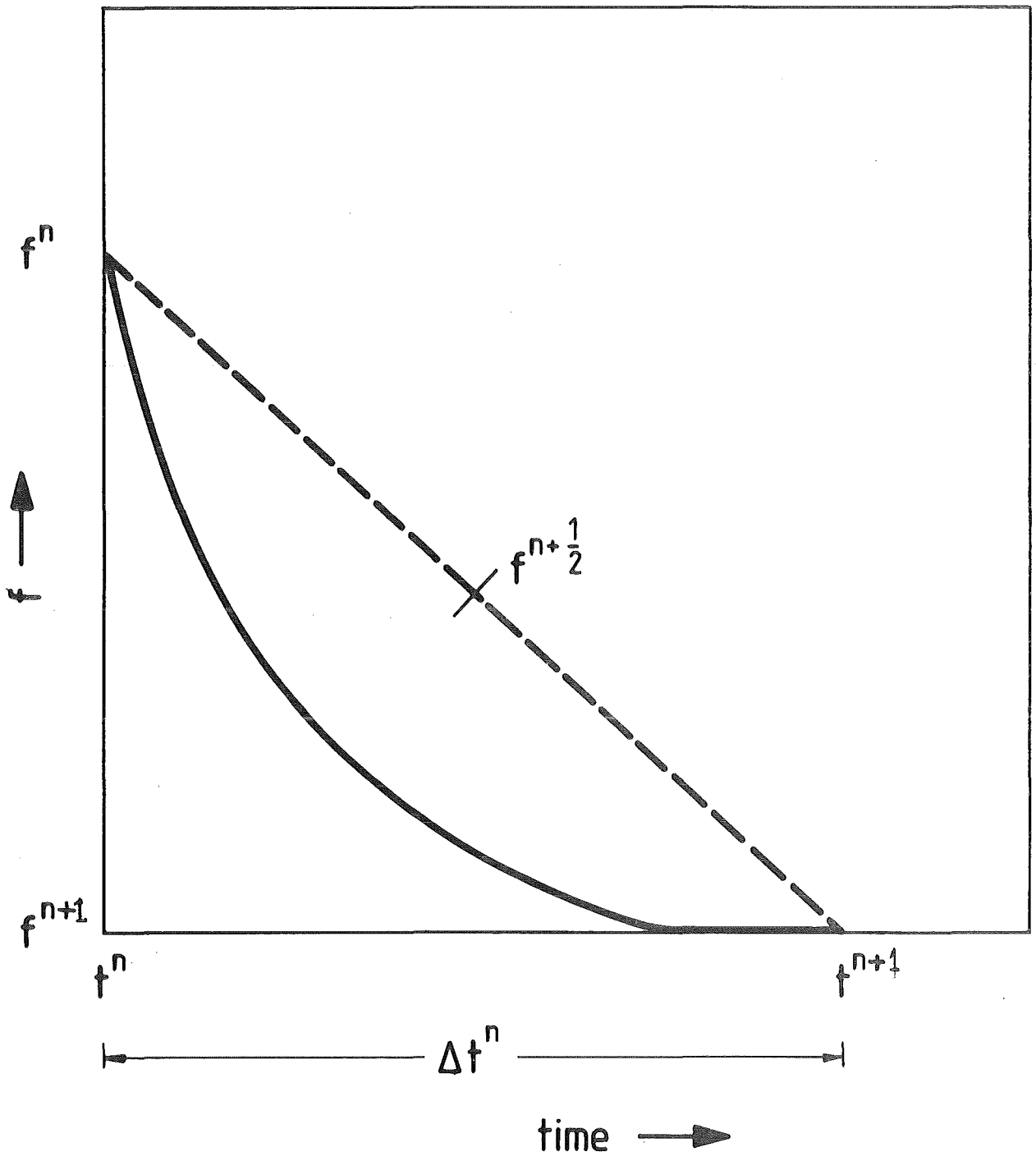

Fig. 3 Decay of f as a function of time

$$f^{n+1/2} = f^{n}\left\langle e^{-\omega t}\right\rangle \tag{2.52}$$

where $$\left\langle e^{-\omega t}\right\rangle = \frac{1}{\Delta t}\int_{o}^{\Delta t} e^{-\omega t}\, dt = \frac{1}{\omega\cdot\Delta t}\left[1 - e^{-\omega\cdot\Delta t}\right] \tag{2.53}$$

In case of ICF plasmas, the electron-ion equipartition time scale τ_{ie} could become many orders of magnitude smaller than the hydrodynamic time scale τ_{hd}. The time-scale of interest in these calculations is τ_{hd} and we cannot afford to restrict the time step by τ_{ie} since it is extremely small. The above technique of analytic fits to the numerical solution is used in MEDUSA to solve this problem and is described below.

The ion and the electron energy equations can be written as

$$\frac{dT_i}{dt} = \frac{W_i}{(C_v)_i} - \frac{K_{ie}}{(C_v)_i} \tag{2.54}$$

$$\frac{dT_e}{dt} = \frac{W_e}{(C_v)_e} + \frac{K_{ie}}{(C_v)_e} \tag{2.55}$$

where W's contain the remaining terms of the energy equations.

Subtracting (2.55) from (2.54) one gets

$$\frac{d}{dt}(T_i - T_e) = \left[\frac{W_i}{(C_v)_i} - \frac{W_e}{(C_v)_e}\right] - \left[\frac{1}{(C_v)_i} + \frac{1}{(C_v)_e}\right] K_{ie} \tag{2.56}$$

where K_{ie} given by (2.23). The above equation can be written as

$$\frac{d\xi}{dt} = \phi - \beta\omega_{ie}\xi \tag{2.57}$$

where $$\xi = T_i - T_e\,, \quad \beta = 1 + \frac{(C_v)_i}{(C_v)_e} \tag{2.58}$$

Assuming ϕ, β and ω_{ie} constant over the time step one can solve (2.57) to get

$$\xi(t) = (\xi_o - \phi/\beta\omega_{ie})e^{-\beta\omega_{ie}t} + \frac{\phi}{\beta\omega_{ie}} \qquad 0 < t < \Delta t \tag{2.59}$$

where $\xi_o = \xi(t=0)$

In a very low density region (2.59) reduces to

$$\xi(t) \simeq \xi_o \tag{2.60}$$

Averaging (2.59) over the time step $\Delta t^{n-1/2}$

$$\xi^{n-1/2} = \left[\xi^{n-1} - \left(\frac{\phi}{\beta\omega_{ie}}\right)^{n-1/2}\right]\left[\frac{1 - e^{-\beta\omega_{ie}^{n-1/2}\cdot\Delta t^{n-1/2}}}{\beta\omega_{ie}^{n-1/2}\Delta t^{n-1/2}}\right] + \left(\frac{\phi}{\beta\omega_{ie}}\right)^{n-1/2} \tag{2.61}$$

Also $$\phi^{n-1/2} = \frac{\xi^n - \xi^{n-1}}{\Delta t^{n-1/2}} + \frac{K_{ie}^{n-1/2}}{(C_v)_i}\beta \tag{2.62}$$

In case of slow exchange rates one uses (2.60) to get

$$\xi^{n-1/2} = \xi^{n-1} \tag{2.63}$$

Heat Conduction Rate:

The rate of energy absorbed in a given cell due to heat conduction is the difference of the rate at which energy flows into that cell and the rate at which it flows out

So $$H_\ell^n = \frac{1}{dM_\ell}\left[F_{j+1}^n - F_j^n\right] \tag{2.64}$$

where $$F_j^n = (R_j^n)^{g-1}\kappa_j^n \frac{T_\ell^n - T_{\ell-1}^n}{R_\ell^n - R_{\ell-1}^n} \tag{2.65}$$

Also $$H_\ell^{n-1/2} = \frac{1}{2}\left[H_\ell^n - H_\ell^{n-1}\right] \tag{2.66}$$

Shock Heating:

The shock heating rate Q can be written as

$$Q_{\ell}^{n-1/2} = - q_{\ell}^{n-1/2} \frac{V_{\ell}^{n} - V_{\ell}^{n-1}}{\Delta t^{n-1/2}} \tag{2.67}$$

where $$q_{\ell}^{n-1/2} = b^2 \rho_{\ell}^{n-1/2} (u_{j+1}^{n-1/2} - u_{j}^{n-1/2}) \tag{2.68}$$

and is only applicable if $u_{j+1} < u_j$.

Method of Solution:

Substituting $H^{n-1/2}$ from eq. (2.64) and (2.65) into eq. (2.44) and collecting the coefficients of $T_{\ell-1}^{n}$, T^{n} and $T_{\ell+1}^{n}$ respectively, we get for the electrons

$$A_{\ell}^{n} T_{\ell-1}^{n} + B_{\ell}^{n} T_{\ell}^{n} + C_{\ell}^{n} T_{\ell+1}^{n} = D_{\ell}^{n} + G_{\ell-1}^{n} \tag{2.69}$$

where we have for the inner boundary $A_1^n = 0$. For the outer boundary we have different conditions for different cases as shown by (2.79) and (2.80).

Where $$A_{\ell}^{n} = - \frac{1}{dM_{\ell}} \frac{(R_j^n)^{g-1} \kappa_j^n}{R_{j+1}^n - R_{j-1}^n} \Delta t^{n-1/2} \tag{2.70}$$

$$C_{\ell}^{n} = - \frac{1}{dM_{\ell}} \frac{(R_{j+1}^n)^{g-1} \kappa_{j+1}^n}{R_{j+2}^n - R_j^n} \Delta t^{n-1/2} \tag{2.71}$$

$$B_{\ell}^{n} = \frac{1}{2} \left[(C_v)_{\ell}^{n-1} + (C_v)_{\ell}^{n} \right] - A_{\ell}^{n} - C_{\ell}^{n} \tag{2.72}$$

$$\begin{aligned} D_{\ell}^{n} = \frac{1}{2} \Big[& (X_{\ell}^{n} + J_{\ell}^{n} + Y_{\ell}^{n} + 2K_{ie,\ell}^{n}) \Delta t^{n-1/2} \\ & - (\rho_{\ell}^{n} - \rho_{\ell}^{n-1}) \left[(B_T)_{\ell}^{n-1} + (B_T)_{\ell}^{n} \right] - (V_{\ell}^{n} - V_{\ell}^{n-1}) \\ & (P_{\ell}^{n-1} + P_{\ell}^{n}) + T_{\ell}^{n-1} \left[(C_v)_{\ell}^{n-1} + (C_v)_{\ell}^{n} \right] \Big] \end{aligned} \tag{2.73}$$

$$G_{\ell}^{n-1} = \frac{1}{2}\,\Delta t^{n-1/2}\left[X_{\ell}^{n-1}+J_{\ell}^{n-1}+Y_{\ell}^{n-1}\right] - C_{\ell}^{n-1}\left[T_{\ell+1}^{n-1}-T_{\ell}^{n-1}\right] + A_{\ell}^{n-1}\left[T_{\ell}^{n-1}-T_{\ell-1}^{n-1}\right] \tag{2.74}$$

One can also write similar expressions for the ion temperature provided that K_{ie} is replaced by $-K_{ie}$ and J and X are replaced by Q.

It is seen from (2.69) that the coefficients A, B, C and D are functions of T_{ℓ}^{n} and therefore (2.69) has to be solved iteratively using Gauss's elimination method for each iteration step. The coefficients G_{ℓ}^{n-1} are known quantities at the previous time level and therefore are not affected by iterations.

For N cells of the simulation mesh we get from (2.69)

$$E_1 = \frac{C_1}{B_1}, \qquad F_1 = \frac{D_1+G_1}{B_1} \tag{2.75}$$

$$E_{\ell} = \frac{C_{\ell}}{B_{\ell} - A_{\ell}E_{\ell-1}}, \qquad F_{\ell} = \frac{D_{\ell}+G_{\ell}-A_{\ell}F_{\ell-1}}{B_{\ell} - A_{\ell}E_{\ell-1}} \tag{2.76}$$

where $\ell = 2, \ldots N$.

And one gets

$$T_N = F_N \tag{2.77}$$

$$T_{\ell} = F_{\ell} - E_{\ell}\,T_{\ell+1} \tag{2.78}$$

where ℓ = N-1, N-2, ... 2,1.

Boundary Conditions:

For cases (a), (c) and (d) of Section 2.2 we use

$$A_1^n \equiv C_N^n \equiv 0 \tag{2.79}$$

For case (b) we set

$$A_1^n = 0$$

$$D_N^n = D_N^n - C_N^n T_{N+1}^n \tag{2.80}$$

where $T_{N+1}^n = T_{N+1}^n(t)$ is the temperature applied at the outer boundary.

Equation of Motion:

The Navier-Stoke's equation (2.41) is solved explicitly and one can write

$$u_j^{n+1/2} - u_j^{n-1/2} = - (R_j^n) g \frac{P_\ell^n - P_{\ell-1}^n + q_\ell^n - q_{\ell-1}^n}{dM_j} \Delta t^n \tag{2.81}$$

and $$dM_j = \frac{1}{2} \left[dM_\ell + dM_{\ell-1} \right] \tag{2.82}$$

The cell boundaries are then moved to new positions as

$$R_j^{n+1} = R_j^n + u_j^{n+1/2} \Delta t^{n+1/2} \tag{2.83}$$

Time Step Control.

As discussed above the equation of motion is solved explicitly and therefore the time step must be restricted by the C.F.L.* condition, namely,

$$\Delta t^{n+1/2} \leq a_1 \text{ Min} \left(\frac{R_{j+1}^n - R_j^n}{c_\ell^n} \right) \tag{2.84}$$

where a_1 is an adjustable parameter ≤ 1 and c_ℓ^n is the speed of sound in cell ℓ at the time level n. Although the energy equations are solved implicitly, for reasons of accuracy, the time variation of T_i and T_e is restricted by an expression of the type

*Courant-Friedrichs-Lewy

$$\Delta t^{n+1/2} \leq a_2 \text{ Min } \left[\frac{T_\ell^{n+1} - T_\ell^n}{T_\ell^{n+1} + T_\ell^n}\right] \Delta t^{n-1/2} \tag{2.85}$$

Similarly we restrict the time step by variation of v. The time step itself is restricted according to

$$\Delta t^{n+1/2} \leq a_o \, \Delta t^{n-1/2} \tag{2.86}$$

The smallest time step which comes out of the above conditions is chosen and convergence of iterations on T_i, T_e and u is examined by

$$\frac{\left|m_u - {}^{m-1}u\right|}{\left|{}^{m}u \quad {}^{m-1}u\right|} = \delta u \tag{2.87}$$

with similar expressions to test convergence of T_e and T_i. In (2.87) m determines the number of iteration and δu should be $\leq 10\%$ to ensure the convergence. Typically up to 5 iterations are required for this purpose.

Calculation of Energies.

At the completion of the time step the energies of the system at level n are calculated

Thermal Energy: $$E_{th}^n = \frac{1}{\gamma - 1} \sum_\ell P_\ell^n \, V_\ell^n \, dM_\ell \tag{2.88}$$

Kinetic Energy: $$E_k^n = \frac{1}{8} \sum_{j \text{ or } \ell} (dM_\ell + dM_{\ell-1}) \tag{2.89}$$

$$\left[(u_j^{n+1/2})^2 + (u_j^{n-1/2})^2\right]$$

The energy input depends on which boundary condition (2.43) has been used.

Case a $$\frac{d}{dt} E_{in}^n = \sum_\ell X_\ell^n \, dM_\ell \tag{2.90}$$

$$\underline{\text{Case b}}: \quad \frac{d}{dt} E_{in}^{n} = \frac{(R_{N+1}^{n})^{g-1}}{R_{N+1}^{n} - R_{N}^{n}} \left\{ \left[\kappa (T_{N+1} - T_{N}) \right]_{i}^{n} + \left[\kappa (T_{N+1} - T_{N}) \right]_{e}^{n} \right\} \tag{2.91}$$

$$\underline{\text{Case c}}: \quad \frac{d}{dt} E_{in}^{n} = \frac{1}{4} (P_{N+1}^{n} + P_{N+1}^{n-1}) \, u_{N+1}^{n-1/2} \left[(R_{N+1}^{n})^{g-1} + (R_{N+1}^{n-1})^{g-1} \right] \tag{2.92}$$

Case d : As case c but with p_{N+1}^{n} replaced by

$$P_{N+1}^{n} = P_{N}^{n} + \frac{1}{2}(q_{N}^{n+1/2} + q_{N}^{n-1/2}) - \frac{1}{2} dM_{N} \frac{u_{N+1}^{n+1/2} - u_{N+1}^{n-1/2}}{\Delta t^{n} (R_{N+1}^{n})^{g-1}} \tag{2.93}$$

The total energy input at level n becomes

$$E_{in}^{n} = E_{in}^{n-1} + \frac{1}{2} \left(\frac{d}{dt} E_{in}^{n} + \frac{d}{dt} E_{in}^{n-1} \right) \Delta t^{n-1/2} \tag{2.94}$$

where $E_{in}^{o} = E_{k}^{o} + E_{th}^{o}$

The energy released by the thermonuclear reactions is

$$E_{f}^{n} = E_{f}^{n-1} + \frac{1}{2} \Delta t^{n-1/2} \sum_{\ell} \left[(Y_{i} + Y_{e})_{\ell}^{n} + (Y_{i} + Y_{e})_{\ell}^{n-1} \right] dM_{\ell} \tag{2.95}$$

The energy E_{neu} carried away by the neutrons is calculated by a similar expression. The Bremsstrahlung radiation loss is

$$E_{b}^{n} = E_{b}^{n-1} + \frac{1}{2} \Delta t^{n-1/2} \sum_{\ell} (J_{\ell}^{n} + J_{\ell}^{n-1}) dM_{\ell} \tag{2.96}$$

The error in the energy calculations is represented by

$$\Delta E^{n} = E_{k}^{n} + E_{th}^{n} - E_{in}^{n} - E_{f}^{n} - E_{b}^{n} \tag{2.97}$$

ΔE is a measure of the truncation errors arising from the use of a finite difference scheme. Finally as a check of the "Lawson criterion" we evaluate

$$\overline{\rho r} = \frac{\int_{o}^{R_o} \rho r \, \rho r^{g-1} dr}{\int_{o}^{R_o} \rho r^{g-1} dr} \tag{2.98}$$

The quantity $\overline{\rho r}$ is proportional to $\overline{n_i \tau}$, where τ is the confinement time of a plasma. We calculate $\overline{\rho r}$ as

$$(\rho R)^n = \frac{\sum_{\ell=1} \rho_\ell^n R_\ell^n \delta M_\ell}{\sum_{\ell=1}^{N} \delta M_\ell} \tag{2.99}$$

$$R_\ell^n = \frac{1}{2} \left[R_{j+1}^n + R_j^n \right] \tag{2.100}$$

2.4 Limitations of the Original Version of MEDUSA

In this section we discuss the limitations of the standard version of the MEDUSA code described in reference /1/.

(a) Target Design.

MEDUSA allows for very simple type of ICF targets, in spherical geometry it can only treat solid micro-spheres. It does not allow handling of hollow shells, multi-layered single and double shell targets.

(b) Atomic Physics.

MEDUSA considers a fixed degree of ionization in the plasma and does not allow for ionization and recombination processes. This assumption is good enough for a D-T plasma which is fully ionized at temperatures of interest to thermonuclear fusion. In case of a medium or high-z target the degree of ionization changes considerably in space and time and therefore it should be evaluated at each time step and in each simulation cell using an appropriate model.

(c) Energy Transport.

In the MEDUSA code, the ions and the thermal electrons are the only means of energy transport from the absorption region to the ablation front. The fast electron and radiation transport are not included. The latter two transport processes are much more important in case of laser-produced ICF plasmas and therefore should be considered in such calculations.

(d) α-particle and Charge Particle Transport.

In the MEDUSA code, the α-particles and other charged particles produced in the thermonuclear reactions deposit their energy locally (at the spot where they are created). In fact these particles travel away from the

point of their origin and deposit their energies to electrons and ions by collisions. In order to simulate these effects one requires to include charge particle transport in the hydrodynamic code.

(e) Neutron Transport.

In very large reactor-size pellets the interaction of the fusion neutrons with the pellet could be important. This requires a proper neutron transport model to be included in MEDUSA.

(f) Equation of State.

The standard version of MEDUSA has only two options for the electron equation of state (EOS), namely, ideal gas and Fermi-degenerate. These two models have limited validity in case of ICF plasmas. One requires more sophisticated models like Thomas-Fermi (TF) and corrected Thomas-Fermi (CTF) for the electrons.

3. Updated Version of MEDUSA at KfK

In this section we describe the updated version of the MEDUSA code which has been used at the Institut für Neutronenphysik und Reaktortechnik (INR), Nuclear Research Centre Karlsruhe to simulate single shell, multi-layered, ion-beam driven reactor-size targets /13,14,15,16,17,18,37/. This version of the code has been developed at the INR and is based on the original version of the MEDUSA code /1/ and on updated versions of this code developed at the University of Glasgow and the Rutherford Laboratory /4,7,9,11/. These latter two versions of the MEDUSA code were developed to allow for additional physical effects and geometrical options which were necessary to simulate laser-compression experiments performed at the Central Laser Facility, Rutherford Laboratory. At the INR we have made additional modifications in order to transform this code to an efficient tool for simulating ion-beam driven inertial confinement fusion targets and we call this version MEDUSA-KA. In section 3.1 and 3.2 we describe changes made to MEDUSA at Glasgow University and the Rutherford Laboratory respectively. In section 3.3 we describe MEDUSA-KA and in section 3.4 the necessary future developments are considered.

3.1 MEDUSA at Glasgow University

At the University of Glasgow the following modifications were made to the code.

Target Design

As explained in Section 2 the standard version of the code can only deal with solid micro-spheres and does not allow for shells or more complicated multi-layered targets. The code was modified by Tahir and Laing /4/ to allow for targets composed of up to three different layers of different materials including mixtures of materials.

Atomic Physics

The original version of MEDUSA does not allow for atomic processes and considers a fixed degree of ionization in the plasma. Since the standard version of MEDUSA was basically written to study very simple type of

targets, namely D-T micro-spheres and the D-T is fully ionized at temperatures of thermonuclear burn, this assumption was valid in that case. With the establishment of the Central Laser Facility at the Rutherford Laboratory, laser-compression experiments were performed using gas filled micro-balloons. Typically the gas used was neon. In this type of target the degree of ionization can change considerably during the implosion. Since the transport coefficients and the thermodynamic properties of the plasma are functions of mean and mean squared ionization, namely, $\langle z \rangle$ and $\langle z^2 \rangle$, it is very important to calculate these two moments at every time step and in each Lagrangian cell of the simulation model. In order to solve this problem, an atomic physics package TRIP(4) /24/ was incorporated into the code by Tahir and Laing /25/. This model is a steady state density and temperature dependent model and it assumes that the plasma is in an ionizational equilibrium due to a balance between collisional ionization and radiative + three-body recombination. The atomic physics rate equations would then reduce to the following set of equations

$$S_{\mu-1} f_{\mu-1} = R_{\mu} f_{\mu} \tag{3.1}$$

where $S_{\mu-1}$ is the rate coefficient for collisional ionization of $(\mu-1)$ times ionized atoms and R_{μ} is the total recombination rate coefficient for μ-times ionized atoms and is given by

$$R_{\mu} = A_{\mu} + n_e B_{\mu} \tag{3.2}$$

In the above equation A_{μ} and B_{μ} are the rate coefficients for radiative and three-body recombination of μ-times ionized atoms respectively.

Solution of (3.1) gives the fraction of μ-times ionized atoms as

$$f_{\mu} = \left[\frac{S_o}{R_1} \cdot \frac{S_1}{R_2} - - - \frac{S_{\mu-1}}{R_{\mu}} \right] f_o \tag{3.3}$$

where f_o is the fraction of atoms in the neutral state. Applying the normalization constraint

$$\sum_{\mu} f_{\mu} = 1 \tag{3.4}$$

one gets

$$f_o = \left[1 + \sum_{\mu} \left| \frac{S_o}{R_o} \cdot \frac{S_1}{R_1} \; - - - - - \; \frac{S_{\mu-1}}{R_\mu} \right| \right]^{-1} \qquad (3.5)$$

One can then evaluate

$$\langle z \rangle = \sum_i i \, f_i \qquad (3.6)$$

and

$$\langle z^2 \rangle = \sum_i i^2 \, f_i \qquad (3.7)$$

The rate coefficients for ionization and recombination are given in the literature /26/. We note that this model includes three-body recombination as well as radiative recombination. The former process is dominant in the core of the laser-pellet whereas the later is important in the corona region. This model therefore reduces to an LTE approximation in the denser part of the target and to a corona equilibrium in the outer underdense region. There is, however, an intermediate region in the pellet in which both these processes are important, therefore neither an LTE model nor a corona model is sufficient to handle that region. Since the TRIP(4) model considers both these effects, it can be applied to that region as shown in reference /7/. The model has also been used to evaluate $\langle z \rangle$ and $\langle z^2 \rangle$ for mixtures of elements like glass which is S_iO_2.

Radiation Transport

The standard version of MEDUSA considers the thermal ions and the thermal electrons to be the only means of energy transport in the plasma. It is, however, well known that the fast electrons and the radiation transport are more important than the thermal ion and the thermal electron transport. The former two processes can transport energy into the target much faster and therefore can preheat the uncompressed target core, thereby degrading the final compression. It is therefore very important to include these two transport mechanisms while simulating laser-compression experiments. A radiation transport package was developed by Tahir and Laing

/4,5,6/ and was coupled into MEDUSA. In this model it is assumed that the radiation field can be described by a local Planckian distribution in a similar manner as the electrons and ions are represented by individual local Maxwellians. The radiation field is characterized by a temperature T_r. The radiation interacts with the electrons as a function of the local temperature difference $(T_e - T_r)$ and it also transports energy in the real space. This equilibrium radiation field can be characterized by the following quantities:

Specific internal energy : $$U_r = \frac{4\sigma T_r^4}{\rho c}$$

Specific heat : $$(C_v)_r = \left[\frac{\partial U_r}{\partial T_r}\right]_\rho$$

Radiation pressure : $$P_r = \frac{1}{3}\rho U_r$$

where the symbols have their usual meaning. This model has been used to study the phenomenon of radiative preheat in different type of targets including solid carbon microspheres and gas-filled microballoons /27,8/.

The model described above is very efficient and it increases the computer run time for a typical problem by a factor of 2. This model however is simple and does not apply accurately in the underdense part of the target. It is therefore desirable to use a multi-group scheme. A multi-group radiation transport scheme has been proposed by Tahir et al. /28/. This scheme treats the problem as a two-dimensional diffusion problem which allows diffusion in the real one-dimensional space as well as in the energy space. It is intended to use ICCG numerical technique /29/ in this package, which would increase the efficiency of the algorithm and hence make it possible to use this package in step with the hydro-dynamics.

3.2 MEDUSA at Rutherford Laboratory

The following modifications were made at the Rutherford Laboratory, Laser Division.

Target Design

MEDUSA was updated at the Rutherford Laboratory independently by Evans /11/ to allow for more complicated types of targets. This version can also deal with layered targets consisting of upto three different layers which can either be a single element or a mixture.

Equation of State

It has been mentioned in Section 2 that the standard version of the MEDUSA code has two options for the electron equation of state, namely, ideal gas (IG) and Fermi-Dirac (FD). These two models however have limited applicability because they do not include some of the essential physics which could be very important in ICF plasmas. Three additional options were provided for the electron EOS in the MEDUSA code by Bell /9/. These options are, a Thomas-Fermi (TF) model, a corrected Thomas-Fermi model (CTF) and a corrected Thomas-Fermi model which simulates the solid density (CTFS). Details of these models are presented in Sec. 3.3.

Atomic Physics (Saha Model)

It is to be noted that although the TRIP(4) method /24,25/ of calculating $\langle z \rangle$ and $\langle z^2 \rangle$ was very accurate, it required a lot of input data to evaluate the rate coefficients for ionization and recombination for all types of ions with different degrees of ionization. The problem becomes even more complicated in case of multi-layered targets and mixture of elements. A simplified Saha equilibrium model was incorporated into MEDUSA by Evans /11/ which calculates $\langle z \rangle$ and $\langle z^2 \rangle$ of the plasma in a very approximate method but is much simpler and more efficient compared to the TRIP(4) method. For further details of this method one should see Zel'dovich and Raizer /30/. This option is called in the MEDUSA code by setting the parameter SAHA = 1.0 in the input list.

Hot Electron Transport

The hot electron transport is one of the very important features of laser-produced plasmas. At the Rutherford Laboratory a hot electron transport package was incorporated into MEDUSA by Evans. This option is still avail-

able in the code for any user who is interested in laser-plasma calculations. For details of this package one should see Ref. /11/.

Ion-Beam Energy Deposition

A simple model was incorporated into MEDUSA by Evans /31/ which can simulate the energy deposition profile of the incident ions. In this model the energy loss formula is given by

$$\frac{1}{E_o}\frac{dE}{dR} = -\frac{N}{R_o}\left[\frac{E}{E_o}\right]^{\frac{N-1}{N}} \quad , \quad \text{where} \quad R = \int_o^d \rho dx$$

ρ is the plasma density, d is the distance into the target, R_o is the range of the incident ions and N is a shape factor.

3.3 MEDUSA at the INR (KfK)

In this section we describe the version of the computer code MEDUSA available at the INR for ion-beam driven ICF targets. This version of the code contains most of the relevant modifications done at the Glasgow University and the Rutherford Laboratory including options for more sophisticated target handling, treatment of atomic processes, additional options for the electron equation of state and simple ion-beam energy deposition formulae. Modifications done at the INR are also included.

In Figs. 4 and 5 we present the physical processes which are important during the compression and burn of an ICF target. At present we do not have incorporated into MEDUSA-KA a number of physical processes shown in these figures, such as radiation transport, more sophisticated treatment for ion-beam energy deposition, transport of charged particles (α-particles, knock-on ions etc.) and transport of neutrons.

It is intended to improve MEDUSA-KA up to the level shown in Figs. 4 and 5, as discussed in section 3.4.

Most of the ICF proposals involve the use of either ion beams (light or heavy) or lasers as the drivers, as shown in Fig. 4. The laser light may have various wavelengths, for instance a CO_2 (10μm) laser, a Nd-Yag (1μm) laser or by use of frequency doubling or tripling much shorter wavelengths

can be obtained. Some laser light is reflected, scattered or refracted from the plasma, for instance by Raman or Brillouin processes. Some of the light is absorbed by inverse Bremsstrahlung until the critical density in the plasma. At this point the laser light is absorbed more or less completely locally by various collective or non-linear processes which are not completely understood. In these processes large amplitude plasma waves and large electric fields are generated which produce high energy suprathermal electrons (50 KeV). These stream into the plasma and lose energy via Bremsstrahlung and Coulomb processes to the electron and radiation fields. Energy is meanwhile also transported into the pellet up to the ablation front by photons and electrons. The 'ablation' of material causes a reaction which implodes the rest of the pellet. From this point on the physical processes are very similar to those that occur in ion beam fusion. We note that the laser light absorption and the hot electron transport treatment are not included in MEDUSA-KA but these routines can be easily reactivated if required.

In ion beam fusion light or heavy ions penetrate deep into the pellet outer layers. Energy is transferred to the electrons and ions of the plasma by Coulomb interactions, nuclear scattering and by the generation of plasmons. It is assumed that no suprathermal particles are created because no instabilities can be identified in such highly collisional plasmas. The energy is transferred mainly to the electrons which then transfer energy on to the ions by electron-ion scattering. Both the ions and electrons conduct heat inwards. The heated ions, and electrons and the radiation emitted by atoms produce a thermal pressure which drives the rest of the pellet (from the end of the ion beam range) inwards. In MEDUSA-KA the energy deposition of the incident ions is simulated using simple analytic formulae. Deposition profile obtained by using these formulae is adjusted by a comparison with a sophisticated code Gorgon /14/ which has not yet been coupled with MEDUSA-KA. In order to treat radiation transport and electron-photon interactions correctly one needs to have good (multigroup or single-group /4/) opacities which take account of such processes as ionization, bound-bound, bound-free, and free-free transitions, and Compton and inverse Compton scattering. These radiation effects are not yet included in MEDUSA-KA. Equation of state data is also required in the equations describing the temperatures (ion and electron) of the plasma and their time development. Hydrodynamic motion in a one-field model is incorporated and the pellet implodes to ignition if sufficient energy is used as input and the right pulse shape which creates the correct carefully timed shocks is used.

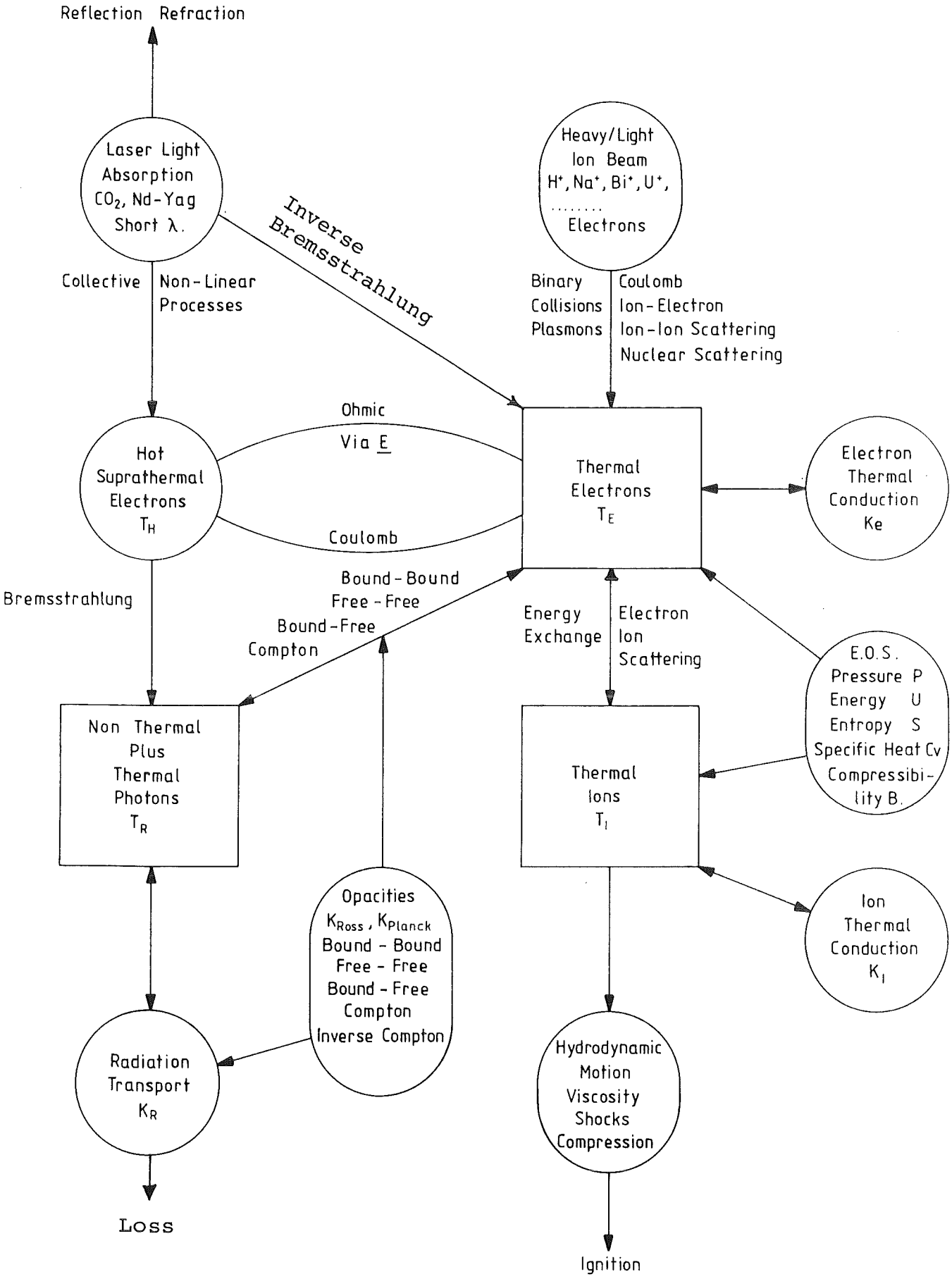

Fig. 4 The important physical processes in the implosion phase of ICF targets

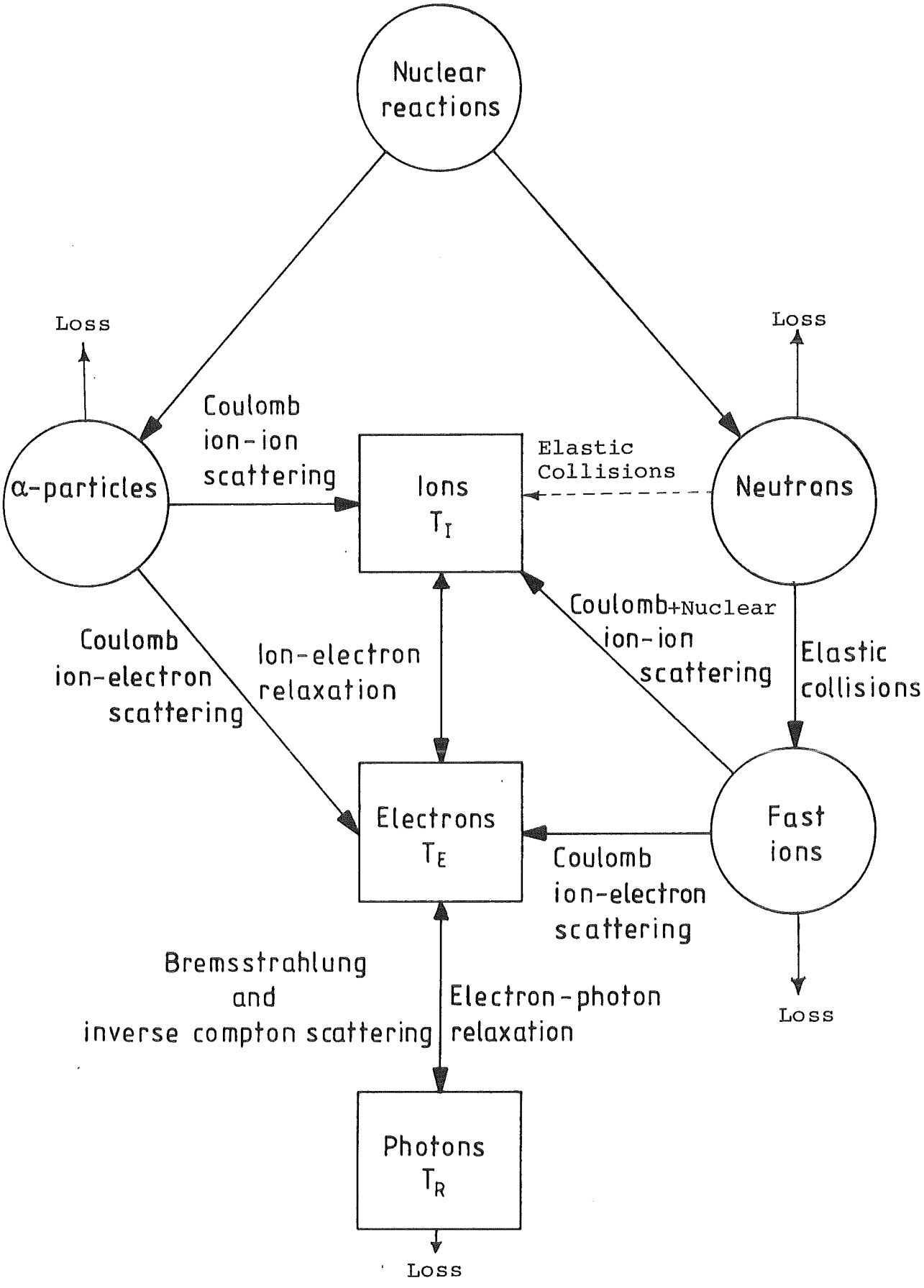

Fig. 5 The important physical processes in the burn of an ICF pellet

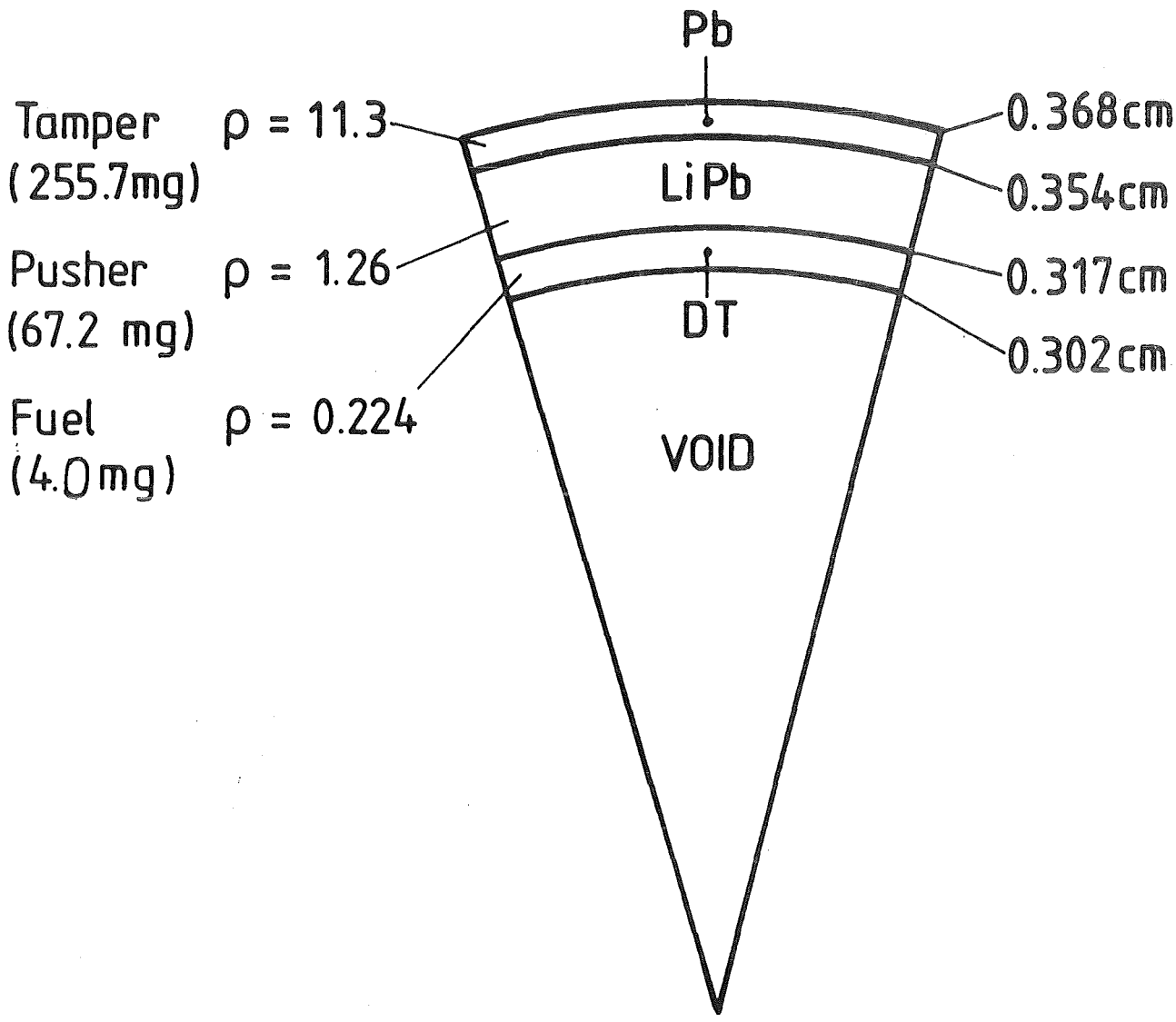

Fig. 6 Target initial conditions

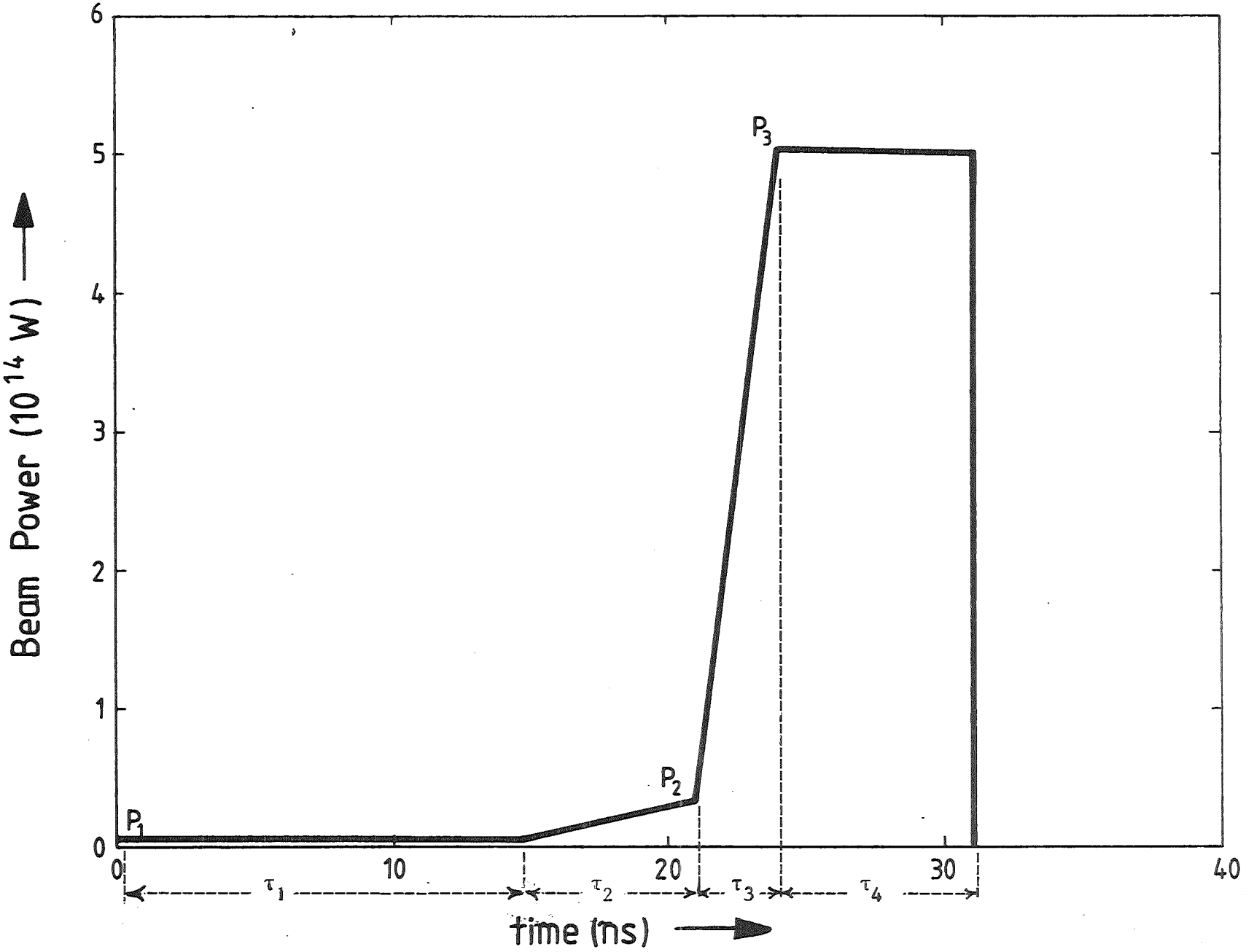

Fig. 7 Input power as a function of time

After ignition nuclear reactions occur and the burn wave spreads throughout the fuel. Neutrons (14.1MeV) and α-particles (3.5MeV) are produced. The neutrons cause 'knock-on' fast ions which together with the α-particles lose energy via Coulomb scattering to the DT plasma. Hence energy is transferred to the ions and electrons which then transfer energy to the radiation field via Bremsstrahlung and inverse Compton scattering. Conduction of heat occurs via electrons, ions and photons. Such processes as hydrodynamic motion also occur during the burn and also input data such as EOS and opacity data are required just as the compression phase. In MEDUSA-KA these processes are not modelled in detail. The α-particles deposit their energy at the point where they are created. The neutrons, on the other hand, are allowed to escape freely.

In the following we discuss the details of the computer code MEDUSA-KA.

Target Initial Conditions

The present version allows for directly driven single shell multi-layered hollow targets like the one shown in Fig. 4. In Fig. 5 Region 1 represents the tamper region which is a high-density, high-z material like Pb. Region 2 is a low-density, low-z pusher region which in our case is Li doped with Pb. The D-T fuel lies in region 3 while the void is region 4.

The initial conditions for this target are set in SUBROUTINE SOURCE in the following manner.

(i) Region 1 (Tamper)

The tamper material is Pb and its physical and chemical properties are described by the following parameters:

Charge number	:	XZ = 82.0
Mass number	:	XMASS = 207.21
Tamper thickness	:	DRTMPR (default = 0.0)
Tamper density	:	ROTMPR (1.13×10^4 kg/m^3)

If DRTMPR is not zero then the chemical composition by a fraction F1X(L) is set equal to unity:

ie F1X(L) = 1.0

where the index L represents all the cells in the tamper region, and are represented by the variable ZTMPR. Some other material like gold can be used instead of Pb by using corresponding XZ and XMASS for that material.

(ii) Region 2 (Pusher)

The pusher material is a mixture of lithium and lead which has a chemical composition $Li_{95}Pb_5$ according to the number density of the atoms. In fact the lithium is doped with lead atoms to stop radiative preheat of the fuel. To evaluate the equation of state (EOS) parameters we replaced the LiPb mixture by an average atom scheme. Our calculations show that the atomic number and the atomic weight of such an atom are equal to 7.0 and 16.48 denoted by XZ1 and XMASS1 respectively. Any mixture of elements can be used provided we replace XZ1 and XMASS1 by those of the new average atom. In the SUBROUTINE SOURCE we preset these quantities as

XZ1 = 7.0
XMASS1 = 16.48

Also other variables are fixed as follows:

Pusher thickness : DRPUSH (default = 0.0)
Pusher density : ROPUSH (1.26×10^3 kg/m^3)

If the pusher thickness is not equal to zero the chemical composition of this region is described by a fraction F1X1(L) which is set equal to 1.0.

ie F1X1(L) = 1.0

where F1X1(L) is the fraction of the average atom and the index L represents all the cells in the pusher region. The total number of mesh points in the pusher is denoted by ZPUSH.

(iii) Region 3 (Fuel Region)

The fuel is a 50-50 mixture of deuterium and tritium atoms and its chemical composition is described by setting

F1T(L) = 0.5
F1D(L) = 0.5

where F1T and F1D represent the fractions of tritium and deuterium respectively.

Fuel thickness : DRFUEL (default = 0.0)
Fuel density : ROFUEL (224.0 kg/m^3)

The number of mesh points in the fuel region are denoted by ZFUEL.

(iv) Region 4 (Void)

Although the void region represents vacuum, we cannot put the density and the temperatures equal to zero in the simulation model, since this would lead to divide checks in the code. To overcome this problem we fill this region with a very low density gas at room temperature such that its pressure is negligibly small. In our simulations we have used hydrogen gas to avoid the complications arising from ionization and recombination in case of a high-z gas. The void region is characterized by the following parameters:

Gas composition : F1H(L) = 1.0
Radius : RINI
Density : RHOINI

We always consider one cell for the void region (the innermost cell of the Lagrangian mesh). Therefore in this case L = 1.

The thermodynamic and hydrodynamic boundary conditions at the outer target boundary are the same as described in Section 2. At the inner boundary the thermodynamic conditions are not changed whereas the hydrodynamic boundary condition has to be modified, as explained in Section 3.6.

Atomic Physics in MEDUSA-KA

MEDUSA-KA was developed to simulate heavy and light ion-beam driven targets which have a complicated multi-layered structure. The targets calculated so far /13,14,15,16,17/ have a high-z tamper made of z. It is therefore very difficult to use TRIP(4) method to evaluate $\langle z \rangle$ and $\langle z^2 \rangle$ for this target as it would require a large amount of additional data. Normally this method is recommended for $z \leq 20$. We therefore have extended the simplified Saha equilibrium model to evaluate $\langle z \rangle$ and $\langle z^2 \rangle$ in our ion-beam targets. Originally in reference /11/ this method could only handle the elements with $z \leq 20$. We extended this package to handle the Pb tamper and also the LiPb pusher. The LiPb mixture is treated by an average atom approach, the atomic number of this atom is 7. Three ionization potentials for this atom are taken for lithium while the remaining four from lead.

Equation of State

Since there are two thermodynamic sub-systems, namely, the ions and the electrons, one needs to specify the equation of state for these two sub-systems. A large part of the treatment of the electron equation of state described in this section is based on Bell's work /9/.

a) Ions:

The ions are considered as a classical perfect gas and their interaction with the electrons is ignored. The following thermodynamic variables are assigned to the ions.

Specific internal energy : $$U_i = \frac{3}{2} \cdot \frac{KT_i}{m_H M} \qquad (3.8)$$

Specific heat : $$(C_v)_i = \frac{3}{2} \cdot \frac{K}{m_H M} \qquad (3.9)$$

Compressibility : $$(B_T)_i = 0.0 \qquad (3.10)$$

Pressure : $$P_i = n_i K T_i \qquad (3.11)$$

where K is the Boltzmann constant, m_H is the proton mass, n_i is the number density of ions and T_i is the ion temperature.

b) Electrons:

The equation of state for the electrons is more complicated as it has a number of options depending on the density and temperature of the plasma. The computer code MEDUSA-KA has the following five options for the electron EOS.

(i) Ideal gas equation of state

In this option the electrons are treated in the same manner as the ions. The electrons are considered to be a system of non-interacting particles which obey Maxwell-Boltzmann statistics having a temperature T_e. Interaction and quantum effects are ignored. The thermodynamic quantities in this model are calculated as follows:

Specific internal energy : $$U_e = \frac{3}{2} \cdot \frac{KT_e}{m_H M} \qquad (3.12)$$

Specific heat : $$(C_v)_e = \frac{3}{2} \frac{K \cdot Z}{m_H M} \qquad (3.13)$$

Compressibility : $$(B_T)_e = 0.0 \qquad (3.14)$$

Pressure : $$P_e = n_e K T_e \qquad (3.15)$$

where n_e is the electron number density and T_e is the electron temperature. In our pellet simulations it is observed that it is easy to compress an ideal gas because there are no repulsive forces. This produces unrealistically large values of the fuel ρR which leads to large gains in the ICF target simulations.

(ii) Fermi-Dirac Equation of State

This model is based on the statistical mechanics of a system of non-interacting particles which obey Pauli's exclusion principle. The pressure in this model is caused by thermal as well as exclusion effects. This is due to the fact that only one such particle can occupy each quantum state. If the number density of the particles is too large then all the low energy states are filled and the remaining electrons have to settle in higher energy states. This costs extra energy and is therefore the origin of very strong repulsive forces in matter. This leads to a zero temperature pressure which is $\propto \rho^{5/3}$. Therefore for a given pressure there is a limit to the amount by which matter can be compressed even at zero temperature. The option for Fermi-Dirac equation of state in MEDUSA-KA uses the following formulae for equation of state variables.

$$(C_v)_e = \frac{3}{2} \cdot \frac{K}{m_H} \cdot \frac{z}{M} \begin{cases} \frac{\pi^2}{3}\xi - \frac{\pi^4}{10}\xi^3 & \xi < \xi_{min} \\ 1 - (6\sqrt{2\pi})^{-1}\,\xi^{-3/2} & \xi_{min} \leq \xi \leq \xi_{max} \\ 1 & \xi_{max} \leq \xi \end{cases} \tag{3.16}$$

$$(B_T)_e = \frac{3}{2} P_F \rho^{-2} \begin{cases} \frac{2}{3} - \frac{5\Pi^2}{18}\xi^2 + \frac{\Pi^4}{8}\xi^4 & \xi < \xi_{min} \\ 5(6\sqrt{2\pi})^{-1}\,\xi^{-1/2} & \xi_{min} \leq \xi \leq \xi_{max} \\ 0 & \xi_{max} < \xi \end{cases} \tag{3.17}$$

$$P_e = \frac{K}{m_H} \cdot \frac{z}{M} \rho T_e \begin{cases} \frac{2}{5}\xi^{-1} + \frac{\Pi^2}{6}\xi - \frac{\Pi^4}{40}\xi^3 & \xi < \xi_{min} \\ 1 + (3\sqrt{2\pi})^{-1}\,\xi^{-3/2} & \xi_{min} \leq \xi \leq \xi_{max} \\ 1 & \xi_{max} \leq \xi \end{cases} \tag{3.18}$$

In the above equations $\xi = T_e/T_F$ where T_F is the Fermi temperature given by (2.9). The parameter ξ determines the degree of degeneracy of the electrons. In case when $\xi > \xi_{max}$ the plasma is non-degenerate. In (3.15) P_F is the Fermi pressure given by

$$P_F = \frac{h^2}{20m_e}\left(\frac{3}{\pi}\right)^{2/3}\left(\frac{z}{m_H M}\right)^{5/3}\rho^{5/3} \qquad (3.19)$$

where the symbols have their usual meaning.

(iii) Thomas-Fermi Equation of State

For a D-T target which is completely ionized above 10 eV, the Fermi-Dirac model is very good. For medium and high-z materials this model is not very accurate as it ignores ionization effects. It also does not take account of the electric field of the nucleus and electrons which is very important in case of high temperature, very dense plasmas. Under the influence of the electrostatic field the electrons and nuclei order themselves into quasi-atoms. Therefore the problem of the equation of state is reduced to solution of the thermodynamic properties of a quasi-atom. At low temperatures and low densities all electrons are confined to lie in the atomic potentials as bound electrons, whereas at high temperatures and high densities some of the electrons can escape and exist as quasi-free electrons. In a Thomas-Fermi model the effective one-electron potential is calculated and then the electrons are distributed within this spherical potential according to Fermi-Dirac statistics. In this model the pressure is much lower at low densities and temperatures compared to the Fermi-Dirac model since in this model there are less free electrons. This option was made available in the MEDUSA code by Bell /9/ at the Rutherford Laboratory. This consists of analytic fits to the Thomas-Fermi graphs of pressure and energy density as a function of density and temperature which were published by Latter /32/. The expressions for the energy and pressure degeneracy curves are taken from March /33/. These analytic fits are given below.

Pressure

$$P1 = 1.602E-12*\frac{T}{V} \tag{3.20}$$

$$P2 = \left(\sum_{N=1}^{5} A(N)*V**(N/6.+0.5)\right)**-2.5 \tag{3.21}$$

$$P3 = (1./(V-0.75E-18*V**-1.75))*(P4**-2.+P5**-2.)**0.5$$

$$+0.75E-18*V**-1.75*P5 \tag{3.22}$$

where $$P4 = A6*T \text{ and } P5 = A7*T**1.61 \tag{3.23}$$

The Thomas-Fermi Pressure is given by

$$PTF = 0.2*P1+P2+0.8*P3 \tag{3.34}$$

Energy

$$U1 = 1.5*T \tag{3.25}$$

$$U2 = A10*AD+A11*SQRT(X0)*PHI**2.5 \tag{3.26}$$

where $$AD = 1./\left(B0*X0**7.772+\sum_{K=1}^{7} B(K)*X0**K\right) \tag{3.27}$$

$$PHI = 1./\left(\sum_{K=1}^{6} C(K)*X0**(K/2)\right) \tag{3.28}$$

```
X0 = 1.324E8*V**0.33333333                                    (3.29)

U3 = (1.E-18*V**-0.75+ALOG(V*1.E22))
     *(A12*T**0.1466+A13*T**-1.0733)**-1.75                   (3.30)

U3 = 1.5*T*T/(1.1+T)                                          (3.31)
```

The Thomas-Fermi energy is given by

```
UTF = 0.2*U1+U2+0.8*(U3+U4)                                   (3.32)
```

Energy Derivatives (Specific heat $(\frac{\partial U}{\partial T})_\rho$)

(i) Temperature

```
DUT1 = 1.5

DUT3 = (1.E-18*V**-0.75+ALOG(V*1.E22))
       *(1.61*A13*T**-2.0733333-0.22*A12*T**-0.853333)
       *(A12*T**0.146666+A13*T**-1.073333)**2.5                (3.33)

DUT4 = 1.5*T*(2.2+T)*(1.1+T)**-2                              (3.34)
```

The temperature derivative of the electron energy for one atom is given by

```
DUDT = 0.2*DUT1+0.8*(DUT3+DUT4)                               (3.35)
```

(ii) Volume (Compressibility $(\frac{\partial U}{\partial \rho})_T$)

```
DUV3 = (1./V-0.75E-18*V**-1.75)
       *(A12*T**0.14666+A13*T**-1.07333)**-2.5)                (3.36)
```

Table 1

A(1)	=	4.486E10
A(2)	=	0
A(3)	=	8.5383E17
A(4)	=	1.3811E21
A(5)	=	5.5707E24
A(6)	=	1.585E-12
A(7)	=	6.760E-13
A(8)	=	3.333E9
A(9)	=	7.627E20
A(10)	=	13.172
A(11)	=	1.7562
A(12)	=	3.283E7
A(13)	=	1.805E8
B(1)	=	0
B(2)	=	0.48705
B(3)	=	0.43462
B(4)	=	6.92013E-2
B(5)	=	5.9472E-2
B(6)	=	-4.9688E-3
B(7)	=	4.3386E-4
C(1)	=	0
C(2)	=	0.48075
C(3)	=	0
C(4)	=	0.06934
C(5)	=	9.7E-3
C(6)	=	3.3704E-3

In the above equations V is the volume occupied by a single atom and U is the energy of one atom. These expressions are correct for a DT plasma but can be used for other elements provided.

V is replaced by Z*V
T is replaced by T*Z**(-4./3.)
P is replaced by P*Z**(-10./3.)
U is replaced by U*Z**(-7./3.)

where Z in this case is the nuclear charge.

(iv) Corrected Thomas-Fermi Model

The Thomas-Fermi model discussed before can be improved by the inclusion of exchange and quantum corrections /34/. These corrections give rise to binding forces which dominate repulsive forces at low temperatures and densities. The overall pressure could then be zero at zero temperature, for a given density. This yields the solid density. As the temperature increases one enters the liquid-gas phase region which cannot be modelled by this method. But as long as one is above the critical temperature of the material under consideration, this problem does not occur.

(v) Corrected Thomas-Fermi Model with Actual Solid Density

The corrected Thomas-Fermi gives the solid density as a function of the nuclear charge. The volume occupied by one atom of the solid is a smooth function of Z, whereas the actual volumes vary in a different manner because of the shell structure of the electrons. It is however possible to adjust the solid density by adjusting the quantum corrections. This option provides a very accurate EOS in MEDUSA-KA and has been used to simulate the HIBALL /13/ targets. It is shown in Figs. 8 and 9 that this EOS option provides an excellent fit to the Los Alamos EOS data /35/ for D-T and Pb. It is to be noted that in a hollow pellet like the one used in the HIBALL study /13/ when the shock breaks through the inner D-T boundary the inner boundary expands in the vacuum and the density of the fuel becomes less than the solid density. In this region the CTF model should be replaced by an ideal gas model. In the code we have made provision that as soon as the density in the inner part of the fuel becomes less than the solid density,

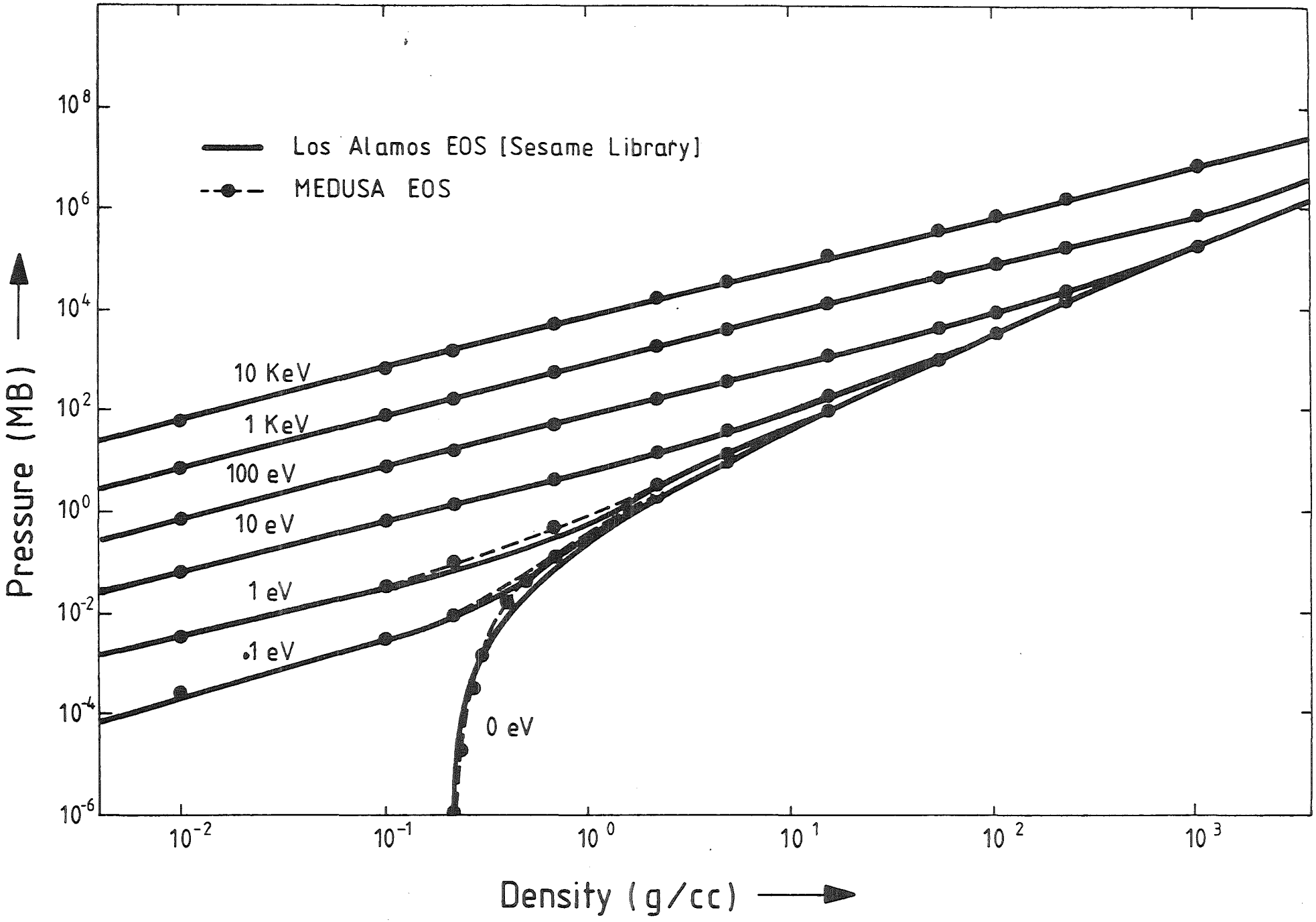

Fig. 8 Equation of state of DT

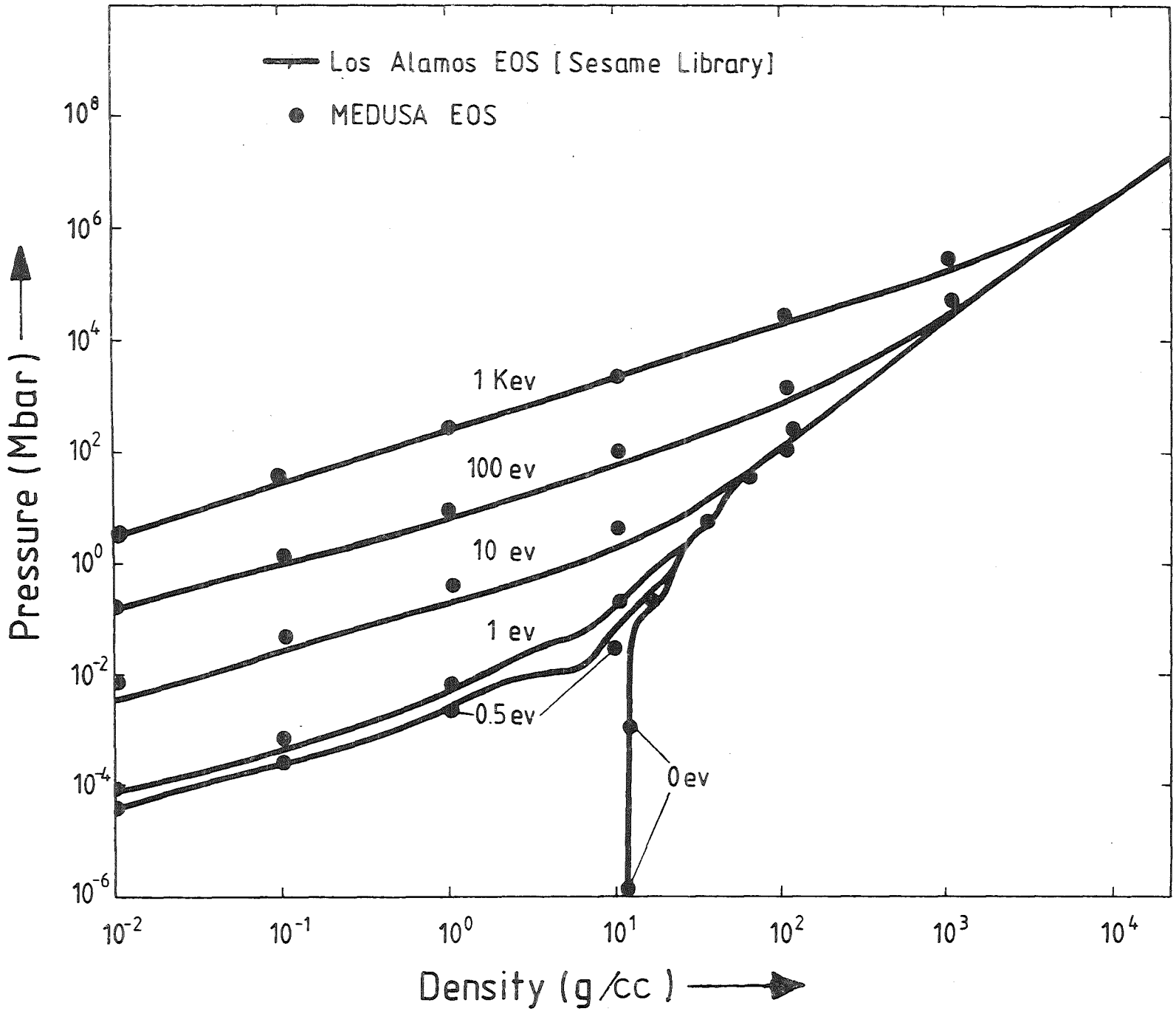

Fig. 9 Equation of state of Pb

she CTF EOS is replaced by an ideal gas EOS. This gives a very good fit to the Los Alamos EOS data in that region, as can be seen from Fig. 8. Whereas in Ref. /9/ the use of CTF EOS for deuterium yields an unphysical behaviour in this low density region.

In the computer code these options are called in the following manner:

For ideal gas EOS for electrons one should set the logical switch

```
NLPFE = .TRUE.
```

in the input data. For any other option one should adjust

```
NLPFE = .FALSE.
```

and then set the variable STATE to any of the following values depending on which option is required.

STATE = 0.0	F-D
STATE = 1.0	T-F
STATE = 2.0	C-T-F
STATE = 3.0	C-T-F with solid density

Energy Deposition

In the standard version of MEDUSA the SUBROUTINE LASER calculates the shape of the laser pulse whereas the absorption of the laser energy is treated in SUBROUTINE ABSORB.In MEDUSA-KA we have replaced these two subroutines by a single SUBROUTINE ABSORB which treats the shape of the input pulse shown in Fig. 7 and also the energy deposition of the input ions in the target material. The energy deposition profile of the incident ions is calculated using analytic formulae (see also /31/) to fit an average deposition profile produced by the energy deposition code Gorgon /14/. These formulae depend on a shape factor and a range factor but do not depend on temperature. Therefore the range shortening effect cannot be modelled by these formulae.

The energy loss formula is given by

$$\frac{1}{E_o}\frac{dE}{dR} = -\frac{N}{R_o}\left[\frac{E}{E_o}\right]^{\frac{N-1}{N}} \tag{3.37}$$

where $R = \int_o^d \rho dx$

ρ is the plasma density, d is the distance into the target, R_o is the range and N is the shape factor. Integrating this formula one gets

$$E(R) = E_o\left[1 - \frac{R}{R_o}\right]^N \tag{3.38}$$

The power $P(R) = n(R) \cdot \frac{1}{2} m v^3(R)$ (3.39)

where n(R) is the density of the ions in the beam, m is the mass of an ion and V(R) is the velocity of the ion. It can be shown that

$$P(R) = P_o\left[1 - \frac{R}{R_o}\right]^N \tag{3.40}$$

By adjusting R_o and N the deposition profile obtained by the above formulae can be made to match a certain profile obtained by the Gorgon code /14/ in the two outer layers of the target.

In the calculation published in references /12,13,14,15,16,17/ the energy deposition profile calculated by using the analytic formulae of equation (3.35) is shown in Fig. 10. This profile is adjusted by a comparison with the energy deposition profile shown in Fig. 11 and which has been obtained by the Gorgon code /14/.

Computational Details

```
ZE(NJP1)=1.0
DO 100 LL=1,NL
L=NLP1-LL
RHOR=RHOR+RHO3(L)*(R3(J+1)-R3(J))
IF(RHOR.GT.RORMAX*0.9999)RHOR=RORMAX*0.9999
```

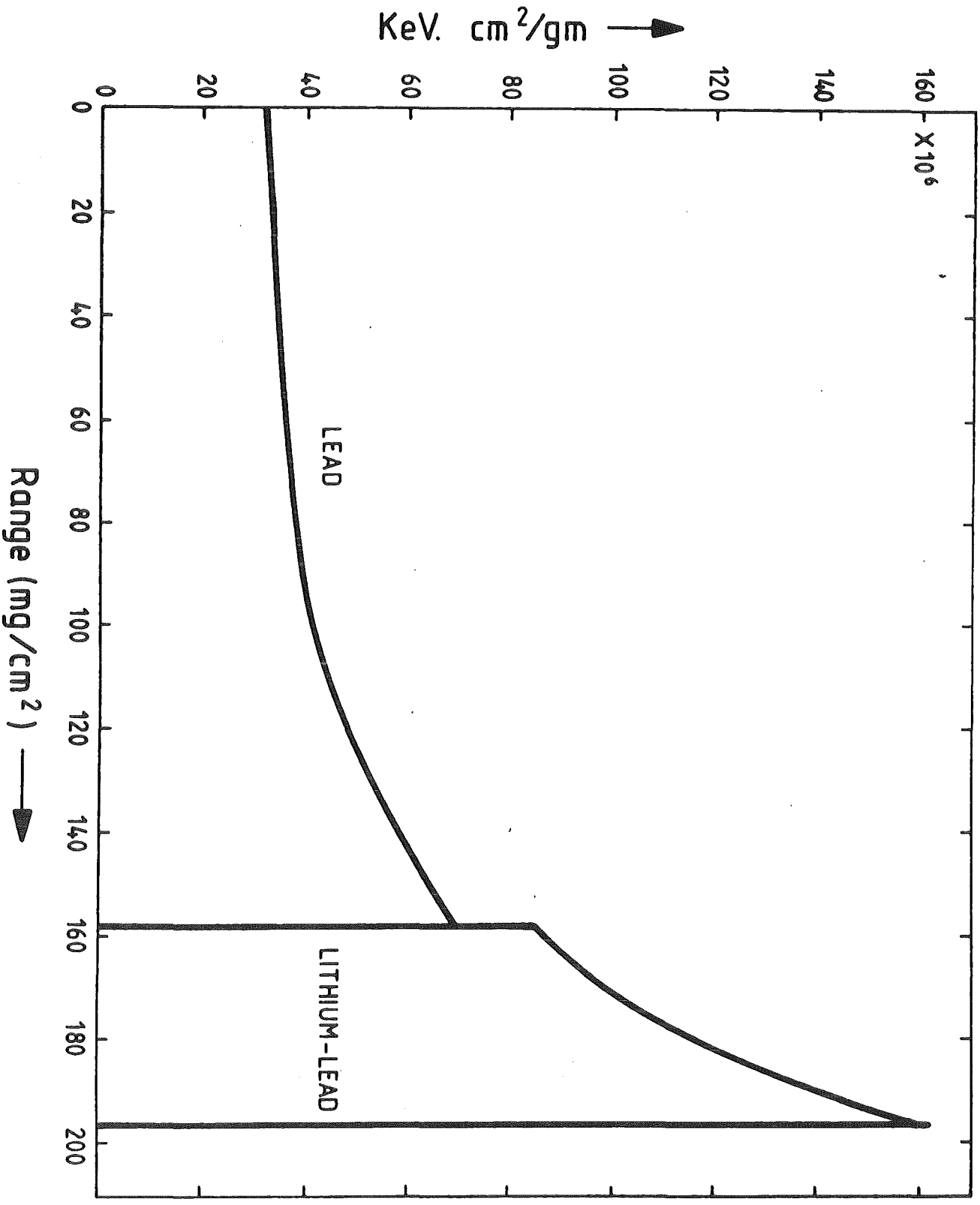

Fig. 10 Energy deposition profile of the incident ions used in the simulations

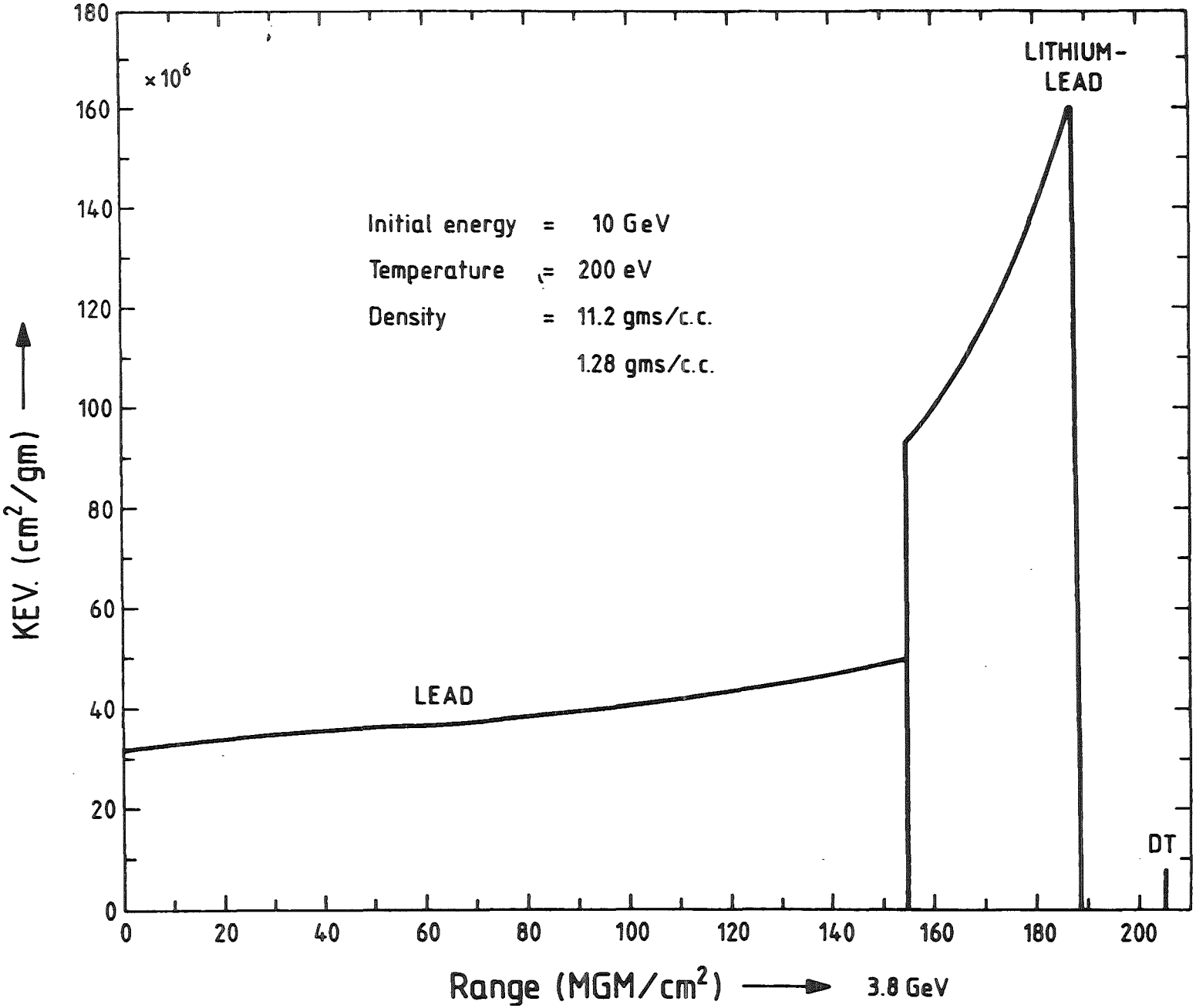

Fig. 11 Energy deposition profile calculated by Gorgon code

```
      ZE(J)=(1.-RHOR/RORMAX)**SHAPE
100   CONTINUE
      NABS1=1
      DO 200 L=1,NL
      J=L
      ZF=ZE(J+1)-ZE(J)
      IF(ZF.EQ.0.0)NABS1=L+1
      XL3(L)=PLAS1*ZF/DM(L)
200   CONTINUE
```

where PLAS1 is the power in the input pulse. By adjusting the SHAPE and the RORMAX variables in the input file one can adjust ZE(J).

Modifications made in the numerics of the code to allow for hollow shells

Boundary conditions:

The hydrodynamic and the thermodynamic boundary conditions at the outer boundary of the target are exactly the same as discussed in Section 2. The thermodynamic boundary conditions at the inner boundary are also the same. However, the hydrodynamic boundary conditions require modifications for the inner boundary in order to allow for the treatment of void. The schematic diagram of the Lagrangian mesh can be drawn as follows.

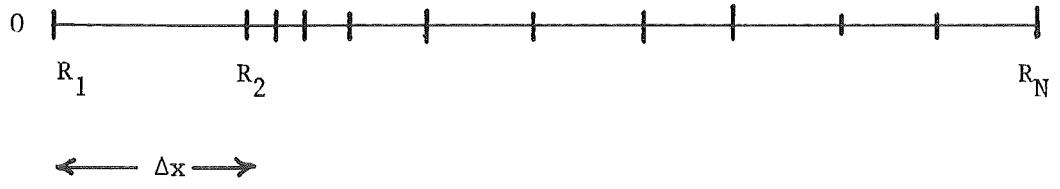

When the first shock breaks through the inner boundary, the co-ordinate R_2 moves towards the origin. As it draws near the origin, Δx decreases. Since there is an extremely low density gas in the void region whose pressure is negligibly small, the thickness Δx can become very small as the void closes. The time step is also restricted by the C.F.L. condition in the first cell (void), namely

$$\Delta t = \frac{\Delta x}{c_s} \tag{3.41}$$

where c_s is the speed of sound in the first cell. Since Δx is very very small, as one approaches void closure the corresponding time step would also be very very small. This is not desirable as it would lead to a waste of the CPU time. To avoid this we removed the restriction on the time step in cell No. 1 in the SUBROUTINE TIMSTP. But this gives rise to an other type of problem. Since these calculations are one-dimensional, a bigger time step would lead to a negative value of R_2, which of course is unphysical. This is resolved by modifying SUBROUTINE MOVEON in the following manner

```
      DO 100 J=1,NJP1
      R5(J)=R3(J)+U4(J)*DT4
100   CONTINUE
      ZZR=5.0E-9
      IF(R5(2).LE.ZZR)R5(2)=ZZR
```

Therefore the inner boundary will be fixed at a distance 5.0×10^{-9} m from the origin which is extremely small.

Also SUBROUTINE CVERGE has been modified to remove convergence checks from the plasma parameters.

3.4 Future Developments

Work is being done at the KfK to update MEDUSA-KA to include the following features which are very important to study the implosion and burn of ICF targets.

(i) Radiation transport

Radiation effects can be very important in compression as well as the burn phase. At present MEDUSA-KA is being updated to include the steady state, one group radiation package /4,5,6/ discussed in Section 3.1. The second stage of this work will be to incorporate the multi-group diffusion model for radiation proposed in /28/.

(ii) Coupling of Gorgon code with MEDUSA

It is desirable to couple the energy deposition code Gorgon /14/ or a simplified version of this code with MEDUSA to allow for temperature dependence and the phenomenon of range shortening in our pellet simulations. This updated version of the code will be a very useful tool to simulate ion-beam plane target experiments which are being planned at the INR for the near future.

(iii) Alpha-particle and charge particle transport

Provisions will be made to MEDUSA-KA to allow for α-particle transport as well as for the transport of other charged particles. This is necessary to see the effect of α-particles on burn propagation and that of the knock on particles produced due to neutron collisions.

(iv) Target design

MEDUSA will be modified to allow handling of more complicated types of targets, e.g. double shell targets.

(v) Inclusion of neutron transport

In large reactor-size targets the neutrons produced in the burning zone of the fuel may re-deposit some energy to the fuel. An escape probability method has been used /19,38/ to treat neutron transport and energy re-deposition in the target. This method is not a part of the MEDUSA-KA version published in this report.

For reactor chamber neutronics the time-dependent behaviour of the neutron spectrum emitted by the target is important. A neutron transport code TIMEX /36/ is being coupled to MEDUSA to study this problem /39/.

4. Instructions for the Users

In this section we provide all the necessary information which a new user would require to operate the computer code MEDUSA-KA available at INR. This includes among other things, an up-to-date list of subroutines, common variables, input variables, input data, equivalences and error messages. In order to make this document self-contained and more easily readable we have also included in this report all the relevant information already described in the standard version of MEDUSA /1/ and references /4,9,11/.

4.1 Input Specification and Output Control

Input Specification:

The input is handled in the MEDUSA-KA by a NAMELIST called NEWRUN. In case the NAMELIST facility is not available one should replace the statement

```
READ(NREAN,NEWRUN)
```

in the SUBROUTINE DATA by a usual FORTRAN READ statement which includes all the variables of the NAMELIST NEWRUN. In the following we provide a complete list of the variables used in the NAMELIST NEWRUN together with their type, default values set in the code and their function.

List of Variables in NEWRUN

Name	Type	Default	Purpose of variable
AK0	R	5.0	Controls ratio of timesteps
AK1	R	0.25	timestep control CFL
AK2	R	0.25	timestep control $\Delta\rho$
AK3	R	0.25	timestep control ΔTi
AK4	R	0.25	timestep control ΔTe
AK5	R	0.0	spare variable, not used.
BNEUM	R	1.0	controls artificial viscosity should not need to be changed.

Name	Type	Default	Purpose of variable
DELTAT	R	1.0E-18	Initial timestep (s)
DEUTER	R	0.5	may be used to obtain non-equimolar DT - see SOURCE
DTEMAX	R	0.1	Convergence criterion Te
DTIMAX	R	0.1	Convergence criterion Ti
DUMAX	R	0.1	Convergence criterion U
GAMMAE	R	1.667	Ratio of specific heats for electrons and ions when perfect gas equation of state is in use.
GAMMAI	R	1.667	
HELIU3	R	0.0	
HELIU4	R	0.0	
HYDROG	R	0.0	
LAMDA1	R	1.0E-5	laser wavelength (m)
NETRAL	R		
NTRLMS	R		
RHOINI	R	124.0	Equivalenced to RHOGAS (kg/m^3)
RINI	R	4.8E-4	Target inside radius (m)
SCP	R	1.0	Scale pressure
SCR	R	1.0	Scale radius
SCRHO	R	1.0	Scale density
SCTE	R	1.0	Scale Te
SCTI	R	1.0	Scale Ti
SCTIME	R	1.0	Scale time
TEINI	R	5.0E3	Initial electron temperature (K)
TIINI	R	5.0E3	Initial ion temperature (K)
TINUCL	R	1.0E7	Minimum ion temperature at which D-T reactions are calculated (K)
TRITIU	R	0.5	Use in conjunction with DEUTER to obtain non-equimolar D-T fill gas.
TSTOP	R	1.0E-6	Maximum simulation time (s)
XMASS	R	0.0	Mass number of extra element
XTRA	R	0.0	Fraction of extra element
XZ	R	0.0	Charge number of extra element
MESH	I	40	Total no. of zones in target
NCASE	I	1	Controls of boundary conditions, defaults to alter illumination.

Name	Type	Default	Purpose of variable
NDUMP	I		
NFILM	I		
NGEOM	I	3	Controls geometry
NHDCPY	I	100	No. of time steps between graphics
NITMAX	I	5	Maximum number of iterations
NP1	I	1	Control lineprinter output
NP2	I	MESH	Control lineprinter output
NP3	I	(MESH/20)	Control lineprinter output
NPRNT	I	100	No. of time steps between lineprinter output.
NREP	I		Controls repetition of cine frames, not used at present.
NLABS	L	TRUE	Switch, inverse Bremsstrahlung
NLBURN	L	TRUE	"Burnup" of fusion fuel.
NLCRIl	L	TRUE	Switch, absorption at critical density
NLDEPO	L	TRUE	Switch, heating by fusion products.
NLDUMP	L		
NLECON	L	TRUE	Switch, electron thermal conduction
NLEMP	L	TRUE	Switch, emergency printing
NLFILM	L		
NLFUSE	L	TRUE	Calculate fusion rates
NLHCPY	L	FALSE	Switch, graphics production
NLICON	L	TRUE	Switch, ion thermal conduction
NLITE	L	TRUE	Switch, iterations
NLMOVE	L	TRUE	Switch, fluid motion
NLPFE	L	TRUE	Switch, electron perfect gas
NLPFI	L	TRUE	Switch ion perfect gas
NLPRNT	L	TRUE	Switch lineprinter output
NLX	L	TRUE	Switch ion-electron relaxation
LASERl	RA(301)	varied but not always useful.	Controls laser specification. See list of equivalences, and pages 65 and 67.
EMID	RA		
NGROUP	I		
NLEDGE	I		Fortran stream numbers
NONLIN	I		for OLMYPUS

Name	Type	Default	Purpose of variable
NOUT	I	6	FORTRAN stream for lineprinter
NPRINT	I		
NIN	I	5	FORTRAN stream for input
NPUNCH			
NRUN	I	1000	Maximum number of timesteps in run
MXDUMP	I		OLYMPUS control of dumping of common blocks, should not be changed.
NADUMP	I		
NPDUMP	I		
NUDUMP	I		
NLCHED	L		
NLHEAD	L		
NLOMT1	LA	F	used to omit subroutines
NLOMT2	LA	F	during execution -
NLOMT3	LA	F	not very useful.
NLREPT	L		
FLIMIT	R	0.0	Electron thermal flux limit
DRFUEL	R	0.0	Thickness of fuel shell (m)
ROFUEL	R	0.0	Density of fuel shell (kg/m^3)
ZFUEL	R	0.0	No. of zones in fuel
FNE	R	0.0	Fraction of neon in fill gas.
FHOT	R	0.0	Fraction of anomalous absorption into hot electrons.
FTHOT	R	0.0	Controls hot electron temperature
ANABS	R	0.0	Fractional anomalous absorption at critical
SAHA	R	0.0	Switch, ionisation equilibrium
STATE	R	0.0	Controls electron equation of state
PONDF	R	0.0	Switch, ponderomotive force
TON	R	0.0	Controls start isentropic laser pulse
PMULT	R	0.0	Controls time of peak of Gaussian laser pulse
ANPULS	R	0.0	No. of Gaussian laser pulses
PLENTH	R	0.0	Laser pulse length
TOFF	R	0.0	Time laser turns off

Name	Type	Default	Purpose of variable
PMAX	R	0.0	Peak laser power
RHOGAS	R	124.0	Gas density in void (kg/m^3)
GAUSS	R	0.0	Switch: laser pulse shape
RHOT	R	0.0	Controls hot electron transport
DRPUSH	R	0.0	Thickness of pusher shell (m)
ROPUSH	R	0.0	Density of pusher shell (kg/m^3)
ZPUSH	R	0.0	No. of zones in pusher shell
DRTMPR	R	0.0	Thickness of tamper shell (m)
ROTMPR	R	0.0	Density of tamper shell (kg/m^3)
ZTMPR	R	0.0	No. of zones in tamper shell

List of EQUIVALENCES

Some elements of arrays LASER1 and PIQ are equivalenced to names which are more physically meaningful for data input only. Internally the names will be those of the array elements.

LASER 1 (1)	:	TON
LASER 1 (2)	:	PMULT
LASER 1 (3)	:	ANPULS
LASER 1 (4)	:	PLENTH
LASER 1 (5)	:	TOFF
LASER 1 (6)	:	PMAX
PIQ (10)	:	FLIMIT
PIQ (11)	:	DRFUEL
PIQ (12)	:	ROFUEL
PIQ (13)	:	ZFUEL
PIQ (14)	:	FNE
PIQ (21)	:	FHOT
PIQ (22)	:	FTHOT
PIQ (37)	:	GAUSS
PIQ (52)	:	ANABS
PIQ (56)	:	PONDF
PIQ (57)	:	RHOT
PIQ (58)	:	SAHA
PIQ (59)	:	STATE
PIQ (61)	:	DRPUSH
PIQ (62)	:	ROPUSH
PIQ (63)	:	ZPUSH
PIQ (64)	:	ZTMPR
PIQ (65)	:	DRTMPR
PIQ (66)	:	ROTMPR
RHOINI	:	RHOGAS

Use of Array LASER1(301)

In order to specify the input pulse parameters shown in Fig. 7 we use the following elements of the array LASER1(301).

LASER1(n)	SUBROUTINE	FUNCTION
LASER 1 (21)		Range factor
LASER 1 (22)		Shape factor
LASER 1 (23)		τ_1 (secs)
LASER 1 (24)	ABSORB	$\tau_1 + \tau_2$ (secs)
LASER 1 (25)		$\tau_1 + \tau_2 + \tau_3$ (secs)
LASER 1 (26)		$\tau_1 + \tau_2 + \tau_3 + \tau_4$ (secs)
LASER 1 (27)		P_1 (W/Steradian)
LASER 1 (28)		P_2 (W/Steradian)
LASER 1 (29)		P_3 (W/Steradian)

Use of Array PIQ

The array PIQ(91) in common block COMADM is used to modify some of the physical processes inside MEDUSA-KA. Most of the variables which need to be set in the data input are all equivalenced to a name which is suggestive of their function. The list below shows the internal use of the array PIQ, for details of how to use the respective elements to modify the physics in the code, refer to the appropriate subroutine.

PIQ(n)	SUBROUTINE	PURPOSE OF VARIABLE
2,3,4,5,6,8	BOUNDY	change boundary conditions
10	HCDUCT	thermal flux limit
11,12,13,14	SOURCE	define target
19,21,22	ABSORB	control laser absorption
20	COULOG	vary ℓn Λ
24	BREMS	vary radiative losses
25	XCHANG	vary e-i relaxation
26,27	HCDUCT	vary thermal conductivity
28,29,10	FUSION	vary fusion processes
31-36	MPRINT	control lineprinter output
37-51	LASER	control pulse shape
52	ABSORB	anomalous absorption
55	SPEED	control boundary conditions
56	FORMP	ponderomotive force
57	ABSORB	hot electron transport
58	IONBAL	control ionisation
59	STATEE	control equation of state
61,62,63,64,65	SOURCE	define target
66		

Output and Numerical Control

NLHCPY logical switch controlling calls to subroutine HDCOPY - the graphics routine

NLFILM logical switch for cine film production, not used at present

NLPRNT logical switch for lineprinter output from subroutine MPRINT

NLEMP controls emergency printing in case the code detects a numerical problem e.g. "iterations fail to converge". Many pages of output are produced so it may be worthwhile to suppress it by setting NLEMP = FALSE.

NLDUMP logical switch for dumping of common blocks to disk or tape for restart purposes - not used at present

NHDCPY, NFILM, NPRNT, NDUMP — number of timesteps between successive production of { Graphics film - not used; lineprinter output; dumps - not used }

NP1, NP2, NP3 control how many mesh points are printed on lineprinter by "WRITE (NOUT, 9999) (R3(J), J=NP1, NP2, NP3)" it is usually worthwhile to set NP3 = 1 otherwise you may get every second or third meshpoint.

NIN, NOUT — FORTRAN stream numbers for default to 5 & 6 respectively { READ; WRITE }

SCP, SCR, SCRHO, SCTE, SCTI, SCTIME — control the units in which quantities appear on the line printer listing for: { pressure; radius; density; electron temperature; ion temperature; time }

Numerical Control

DELTAT intial timestep, defaults to 10^{-18} sec, the code will quickly settle down to its own choice.

AKO controls maximum allowable ratio of successive timesteps. Set AKO to something large, e.g. 100.0 if message "time centering is damaged" appears.

AK1, AK2, AK3, AK4, AK5 — these numbers control the choice of timestep by the code, refer to routine TIMSTP. AK1 controls the CFL condition: $\Delta t < \frac{\Delta r}{c_s}$. AK2, AK3, AK4 control rate of change of density, ion temperature and electron temperature respectively, AK5 is not used at present.

NLITE — logical switch for interations on T_i, T_e, U. Since the thermal conductivity is non-linear it is best to iterate. Calculations which have electron thermal conduction switched off could set NLITE = FALSE.

DUMAX, DTEMAX, DTIMAX — fractional change in U, T_e, T_i which represents acceptable convergence

NITMAX — Maximum no. of iterations before code stops with message 'iterations fail to converge'

MEDUSA error messages

There are two fairly common error messages:

a) TIME CENTERING DAMAGED means that the ratio of successive time steps is less than $(AK0)^{-1}$. Remedy is to make AK0 larger, say 100.0 or even 1.0E4. There is no penalty in run time and only a small likelihood of serious numerical error.

b) ITERATIONS FAIL TO CONVERGE VARIABLE n CELL ℓ.
This is self-explanatory, the variable n take the values
1 velocity
2 density (specific volume)
3 Ti
4 Te

The cure here is to reduce the value of AKn (i.e. AK4 if Te fails to converge) to a smaller value. 0.15 is usually satisfactory but some times 0.1 is necessary. There is an increase in run time as the various AKn are reduced but the magnitude of this is unpredictable.

There are also messages DENSITIES too low and TEMPERATURES too low, these are usually associate with runs in which the simulation time has exceeded 10^{-6} sec and further running is pointless anyway.

4.2 List of Subroutines

No.	Name	Purpose of Subroutine
1	LABRUN	Label the run
2	CLEAR	Clear variables and arrays
3	PRESET	Set default values
4	DATA	Define data specific to the run
5	AUXVAL	Set auxiliary variables
6	INITAL	Define physical initial conditions
7	START	Prepare to start the calculations
8	SOURCE	Change standard initial conditions
9	CHINIC	Check initial conditions
10	STEPON	Step on the calculations
11	MOTION	Controls the motion
12	LASER(1)	Produces the laser power
13	GIE	Terms of the energy equation at level n - 1
14	STIT	Starts iterations by assuming level 1 = 3
15	STATEI(K)	Describes state of ions
16	STATEE(K)	Describes state of electrons
17	COULOG	Evaluates Coulomb's logarithm
18	ABSORB	Evaluates absorption of laser light
19	BREMS	Radiation loss rate due to Bremsstrahlung
20	XCHANG(K)	Electron-ion energy exchange
21	FUSION	Energy released due to thermonuclear reactions
22	HCDUCT	Thermal conductivities
23	ABCD	Calculates A, B, C, D
24	FINDT	Calculates T
25	TIMSTP	Determines the time step
26	SPEED	Hydrodynamic velocities
27	NEUMAN	Viscous pressure
28	MOVEON	Advances Lagrangian co-ordinate
29	VOLUME	Volumes and densities
30	CVERGE	Checks the convergence of T_i, T_e and U
31	ENERGY	Calculates relevant energies
32	SHIFT	Shifts the levels 1 - 5 back
33	FORMP	Hydrodynamic pressure

No.	Name	Purpose of Subroutine
34	BOUNDY(K)	Sets the boundary value
35	EXAM	Examines present state of the system
36	REVERS	Reverse the calculations if program breaks down
37	BURNUP	Burn-up of Deuterium-Tritium
38	OUTPUT(K)	Output control
39	MPRINT(K)	Main printing routine
40	SELECT	Selects the output
41	TESEND	Tests for completion of run
42	ENDRUN	Terminate the run
43	REPORT(3)	Reports diagnostic information
44	CLIST(2)	Print common variables
45	ARRAYS(2)	Print common arrays
46	HDCOPY(K)	Production of graphics (dummy)

The following subroutines have been modified or added to the MEDUSA code in order to transform it to an ion-beam ICF code MEDUSA-KA.

No.	Name	Purpose of Subroutine
1	SOURCE	To set initial conditions for a single shell, multi-layered reactor-size hollow target
2	DATA	To allow for extra data in the name list
3	ABSORB	To account for incident ion energy deposition
4	CVERGE	To remove convergence check in the void region
5	TIMSTP	To remove time step restrictions in the void cell
6	IONBAL	Calculates ionization level in the plasma
7	SAHA	Evaluates Saha equilibrium for high-z material (Pb)
8	MOVEON	To allow treatment of the inner boundary at void closure
9	SAHA1	Evaluates Saha equilibrium for $z \leq 20$

4.3 List of the Common Blocks

No.	Name	Contents
1	COMBAS	Basic system parameters (OLYMPUS)
2	COMDDP	Diagnostics and program development (OLYMPUS)
3	COMHYD	Hydrodynamics
4	COMTH	Thermodynamics
5	COMIE	Ions and electrons
6	COMLAS	Laser variables
7	COMFUS	Thermonuclear fusion
8	COMEN	Energies
9	COMCON	Physical control
10	COMNC	Numerical control parameters
11	COMNUM	Mesh and numerical methods
12	COMADM	Administrative variables
13	COMOUT	Input-output variables

4.4 List of the Common Variables

In this sub-section we provide a list of all the common variables together with their function. We have changed the dimensions of the common arrays from 91 to 301 in order to allow for more space cells in the target region. This would prove very useful to modify the code for double shell targets.

OLYMPUS Common Blocks

Common Block Name	Variable Name	Type	Purpose of Variable
COMBAS	ALTIME	R	Time allocated to JOB
	CPTINE	R	CPU time used so far on the Job
	NLEDGE	L	Channel for restart records
	NLEND	L	.TRUE. if run to be terminated
	NLRES	L	.TRUE. if run to be restarted
	NONLIN	I	Channel for online input-output
	NOUT	I	Current output channel
	NPRNT	I	Channel for printed output
	NREAD	I	Channel for card input
	NREC	I	Current record number
	NRESUM	I	Resume from record on this channel
	NSTEP	I	Current step number
	STIME	R	Start time
	LABEL1	RA	Label describing the run
	LABEL2	RA	Label describing the run
	LABEL3	RA	Label describing the run
	LABEL4	RA	Label describing the run
	LABEL5	RA	Label available to programmer
	LABEL6	RA	Label available to programmer
	LABEL7	RA	Label reserved for system use
	LABEL8	RA	Label reserved for system use
	NDIARY	I	Channel for diary
	NIN	I	Current input channel
	NPUNCH	I	Channel for card output
	NRUN	I	Maximum number of steps

Common Block Name	Variable Name	Type	Purpose of Variable
COMDDP	MAXDUM	I	Maximum dimension of dump arrays
	MXDUMP	I	Actual dimension of dump arrays
	NADUMP	I	Codes for arrays dumps
	NCLASS	I	Most recent class records
	NPDUMP	I	Codes for dumping points
	NPOINT	I	Most recent point reported
	NSUB	I	Most recent subprogram reported
	NVDUMP	I	Codes for dumping variables
	NLCHED	L	.TRUE. If 0 class report heads required
	NLHEAD	L	.TRUE. If 1-9 class report heads required
	NLOMT1	L	Class 1 subprogram selector
	NLOMT2	L	Class 2 subprogram selector
	NLOMT3	L	Class 3 subprogram selector
	NLREPT	L	Class 4 subprogram selector

MEDUSA Common Blocks

COMHYD	DM	RA	Cell masses
	P3	RA	Hydrodynamic pressure at level 3
	PINI	R	Initial hydrodynamic pressure
	R1	RA	Coordinates of cell boundaries at level 1
	R3	RA	Coordinates of cell boundaries at level 3
	R5	RA	Coordinates of cell boundaries at level 5
	RHO1	RA	Physical density at level 1
	RHO3	RA	Physical density at level 3
	RHO5	RA	Physical density at level 5
	RHOINI	R	Initial value of RHO
	RHOR	R	Integral of RHO * R
	RINI	R	Initial dimension of system
	TIME	R	The real time in the calculation
	U2	RA	Hydrodynamic velocities at level 2
	U4	RA	Hydrodynamic velocities at level 4

Common Block Name	Variable Name	Type	Purpose of Variable
	UEDGE	R	Boundary velocity at level 3
	V1	RA	Specific volumes at level 1
	V3	RA	Specific volumes at level 3
	V5	RA	Specific volumes at level 5
COMTH	DDROE1	RA	Partial derivative of electron energy
	DDROE3	RA	Partial derivative of electron energy
	DDROI1	RA	Partial derivative of ion energy
	DDROI3	RA	Partial derivative of ion energy
	DDTE1	RA	Partial derivative of electron energy
	DDTE3	RA	Partial derivative of electron energy
	DDTI1	RA	Partial derivative of ion energy
	DDTI3	RA	Partial derivative of ion energy
	GAMMAE	R	Ratio of specific heats (electrons)
	GAMMAI	R	Ratio of specific heats (ions)
	KAPPAE	RA	Electron thermal conductivity
	KAPPAI	RA	Ion thermal conductivity
	PE1	RA	Electron pressure at level 1
	PE3	RA	Electron pressure at level 3
	PI1	RA	Ion pressure at level 1
	PI3	RA	Ion pressure at level 3
	TE1	RA	Electron temperature at level 1
	TE3	RA	Electron temperature at level 3
	TEINI	R	Initial electron temperature
	TI1	RA	Ion temperature at level 1
	TI3	RA	Ion temperature at level 3
	TIINI	R	Initial ion temperature
COMIE	BREMS1	RA	Rate of Bremsstrahlung at level 1
	BREMS3	RA	Rate of Bremsstrahlung at level 3
	DEGEN	R	Degree of electron degeneracy
	DEGMAX	R	Upper limit of partial degeneracy
	DEGMIN	R	Lower limit of partial degeneracy
	EFFZ	RA	Average charge number
	FZ1	RA	Average charge at level 1
	FZ3	RA	Average charge at level 3

Common Block Name	Variable Name	Type	Purpose of Variable
	FZSQ1	RA	Average Z*Z at level 1
	FZSQ3	RA	Average Z*Z at level 3
	EIXCH2	RA	Rate of ion-electron energy exchange
	LC	RA	The Coulomb logarithm
	MIEFF	RA	Average ion mass number
	NE	RA	Electron number density
	NI	RA	Number density of ions and neutrals
	OMEGA1	RA	Time rate of ion-electron energy exchange
	PMASS	R	Proton mass
COMLAS	ALPHA1	RA	Absorption coefficient
	ELAS1	R	Current laser energy deposited
	LAMDA1	R	Wave-length of laser light
	LASER1	R	Description of laser pulse
	PLAS1	R	Laser power as a function of time
	RABS1	R	Coordinate with critical density
	ROCRI1	R	Critical density value for absorption
	NECRI1	R	Critical electron density
	XL1	RA	Rate of energy absorbed at level 1
	XL3	RA	Rate of energy absorbed at level 3
	NABS1	I	Number of cell with critical density
COMFUS	DEUTER	R	Initial deuterium fraction
	F1D	RA	Fraction of deuterium at level 1
	F3D	RA	Fraction of deuterium at level 3
	F1H	RA	Fraction of hydrogen at level 1
	F3H	RA	Fraction of hydrogen at level 3
	F1HE3	RA	Fraction of helium3 at level 1
	F3HE3	RA	Fraction of helium3 at level 3
	F1HE4	RA	Fraction of helium4 at level 1
	F3HE4	RA	Fraction of helium4 at level 3
	F1NEU	RA	Fraction of neutrons released at level 1
	F3NEU	RA	Fraction of neutrons released at level 3
	F1NTRL	RA	Fraction of neutrals at level 1
	F3NTRL	RA	Fraction of neutrals at level 3

Common Block Name	Variable Name	Type	Purpose of Variable
	F1T	RA	Fraction of tritium at level 1
	F3T	RA	Fraction of tritium at level 3
	F1X	RA	Fraction of an extra element at level 1
	F3X	RA	Fraction of an extra element at level 3
	HELIU3	R	Initial fraction of helium3
	HELIU4	R	Initial fraction of helium4
	HYDROG	R	Initial fraction of hydrogen
	NETRAL	R	Initial fraction of neutrals
	NTRLMS	R	Mass number of neutral element
	PNEUT1	R	Neutron power at level 1
	PNEUT3	R	Neutron power at level 3
	R1DD	RA	Number of D-D reactions at level 1
	R3DD	RA	Number of D-D reactions at level 3
	R1DHE3	RA	Number of D-HE3 reactions at level 1
	R3DHE3	RA	Number of D-HE3 reactions at level 3
	R1DT	RA	Number of D-T reactions at level 1
	R3DT	RA	Number of D-T reactions at level 3
	RNEUT1	R	Neutron flux at level 1
	RNEUT3	R	Neutron flux at level 3
	TINUCL	R	Lower threshold for thermonuclear reactions
	TOTNEU	R	Total number of neutrons released
	TRITIU	R	Initial fraction of tritium
	XMASS	R	Mass number of extra element
	XTRA	R	Initial fraction of extra element
	XZ	R	Charge number of extra element
	YE1	RA	Fusion energy apportioned to electrons
	YE3	RA	Fusion energy apportioned to electrons
	YI1	RA	Fusion energy apportioned to ions
	YI3	RA	Fusion energy apportioned to ions
	YIELD	R	Ratio of thermonuclear/laser energies

Common Block Name	Variable Name	Type	Purpose of Variable
	XZ1	R	Charge number of extra element
	XZ2	R	Charge number of extra element
	XZ3	R	Charge number of extra element
	XZ4	R	Charge number of extra element
	XMASS1	R	Mass number of extra element
	XMASS2	R	Mass number of extra element
	XMASS3	R	Mass number of extra element
	XMASS4	R	Mass number of extra element
	F1X1	RA	Fraction of extra element at level 1
	F3X1	RA	Fraction of extra element at level 3
	F1X2	RA	Fraction of extra element at level 1
	F3X2	RA	Fraction of extra element at level 3
	F1X3	RA	Fraction of extra element at level 1
	F3X3	RA	Fraction of extra element at level 3
	F1X4	RA	Fraction of extra element at level 1
	F3X4	RA	Fraction of extra element at level 3
COMEN	EEFUSE	R	Thermonuclear energy given to electrons
	EERROR	R	Error in the energy calculation
	EIFUSE	R	Thermonuclear energy given to ions
	EINDT1	R	Energy input at level 1
	EINDT3	R	Energy input at level 3
	EINPUT	R	Total energy input
	ELOSS	R	Total energy loss through radiation
	EN	R	Total energy of system
	ENEUTR	R	Total energy of escaping neutrons
	PV	R	Total thermal energy of system
	USQM	R	Total kinetic energy of system
COMCON	PMIN	R	Permissible minimum of pressure
	RHOMIN	R	Permissible minimum of density
	TEMIN	R	Permissible minimum of electron temperature
	TIMIN1	R	Permissible minimum of ion temperature
	UMIN	R	Smallest velocity allowed for safety

Common Block Name	Variable Name	Type	Purpose of Variable
	MSTEP	I	Timestep counter
	NCASE	I	Selects boundary conditions
	NGEOM	I	Selects the geometry
	MLBRMS	L	Program switch for Bremsstrahlung
	MLECON	L	Program switch for electron heat conduction
	MLFUSE	L	Program switch for thermonuclear reactions
	MLICON	L	Program switch for ion heat conduction
	MLX	L	Program switch for I-E exchange
	NLABS	L	Switch: Absorption by inverse Bremsstrahlung
	NLBRMS	L	Switch: Bremsstrahlung
	NLBURN	L	Switch: Burn-up of D and T
	NLCRIl	L	Switch: Dump laser power at ROCRIl
	NLDEPO	L	Switch: Deposit thermonuclear energies
	NLECON	L	Switch: Electron thermal conduction
	NLFUSE	L	Switch: Thermonuclear reactions
	NLICON	L	Switch: Ion thermal conduction
	NLMOVE	L	Switch: Hydrodynamic motion
	NLPFE	L	Switch: Perfect electron gas laws
	NLPFI	L	Switch: Perfect ion gas laws
	NLX	L	Switch: Ion-electron energy exchange
COMNC	AK0	R	Control the time centering
	AK1	R	Control DT by soundspeed
	AK2	R	Control DT by variations in volume
	AK3	R	Control DT by variations in TI
	AK4	R	Control DT by variations in TE
	AK5	R	Spare DT control parameter
	BNEUM	R	Determines the rate of shock heating
	DELTAT	R	User specifies value of DT
	DT2	R	Timestep (T3 - T1)
	DT3	R	Timestep (T4 - T2)
	DT4	R	Timestep (T5 - T3)

Common Block Name	Variable Name	Type	Purpose of Variable
	DTEMAX	R	Controls convergence of TE
	DTIMAX	R	Controls convergence of TI
	DTMAX	R	Maximum value of DT
	DTMIN	R	Minimum value of DT
	DUMAX	R	Controls of convergence of U
	RDT2	R	= 1.0 / DT2
	RDT3	R	= 1.0 / DT3
	RDT4	R	= 1.0 / DT4
	NCELDT	I	The cell number that sets the limit of DT
	NCONDT	I	Condition determining DT
	NIT	I	Current number of iterations
	NITMAX	I	Maximum number of iterations allowed
	BREAK	L	Break the calculation
	NLGOON	L	Iterations converge
	NLITE	L	Switch: Solve equations by iterations
COMNUM	AE	RA	Coefficient in electron energy equation
	AI	RA	Coefficient in ion energy equation
	BE	RA	Coefficient in electron energy equation
	BI	RA	Coefficient in ion energy equation
	CE	RA	Coefficient in electron energy equation
	CI	RA	Coefficient in ion energy equation
	DE	RA	Coefficient in electron energy equation
	DI	RA	Coefficient in ion energy equation
	E	RA	Auxiliary array used for Gauss elimination
	F	RA	Auxiliary array used for Gauss elimination
	GE	RA	Coefficient in electron energy equation
	GI	RA	Coefficient in ion energy equation
	Q2	RA	Viscous pressure at level 2
	Q4	RA	Viscous pressure at level 4
	TEITE	RA	Level 3 value of TE from previous iteration

Common Block Name	Variable Name	Type	Purpose of Variable
	TIITE	RA	Level 3 value of TI from previous iteration
	UITE	RA	Level 4 value of U from previous iteration
	MESH	I	Number of cells in mesh
	NJ	I	Auxiliary variable (=NJP1-1=MESH)
	NJM1	I	Auxiliary variable (=NJ-1)
	NJP1	I	Number of cell boundaries (=MESH+1)
	NL	I	Number of cells in mesh (=MESH)
	NLM1	I	Auxiliary variable (=NL-1)
	NLP1	I	Auxiliary variable (=NL+1)
COMADM	PIQ	RA	General purpose array
	TSTOP	R	Maximum value of time permitted
	MAXDIM	I	Maximum permissible mesh size
	MAXRUN	I	Maximum number of timesteps permitted
	NDUMP	I	Frequency of dumping common areas
	NREP	I	Repetition of film frames
	NLDUMP	L	Switch: Dumping of common areas
	NLEMP	L	Switch: Emergency printing
COMCUT	BUF1	RA	Output buffer (R)
	BUF2	RA	Output buffer (u)
	BUF3	RA	Output buffer (density)
	BUF4	RA	Output buffer (pressure)
	BUF5	RA	Output buffer (ion temperature)
	BUF6	RA	Output buffer (electron temperature)
	SCP	R	Input-output scaling factor for pressure
	SCR	R	Input-output scaling factor for coordinates
	SCRHO	R	Input-output scaling factor for density
	SCTE	R	Input-output scaling factor for TE
	SCTI	R	Input-output scaling factor for TI
	SCTIME	R	Input-output scaling factor for time
	NFILM	L	Frequency of film frame production

Common Block Name	Variable Name	Type	Purpose of Variable
	NHDCPY	I	Frequency of hardcopy production
	NP1	I	Array printing selector: Start
	NP2	I	Array printing selector: End
	NP3	I	Array printing selector: Increment
	NPRNT	I	Frequency of printing
	NLFILM	L	Switch: Film production
	NLHCPY	L	Switch: Hardcopy production
	NLPRNT	L	Switch: Printing

5. Extended Test Problem

In order to illustrate the use of this updated version of the code we describe a test problem. This problem concerns with the implosion, ignition and burn of a single shell, multi-layered, reactor-size target which is driven by beams of heavy ions /13,14,15/. The target initial conditions are shown in Fig. 6 and the time history of the input power is given in Fig. 7.

5.1 Input Data

```
C     TEST RUN FOR MEDUSA-KA
C     HEAVY ION-BEAM DRIVEN
C     REACTOR-SIZE SINGLE SHELL
C     MULTI-LAYERED HOLLOW PELLET
      &NEWRUN
      DELTAT = 1.0E-18,
      RINI = 3.02E-3,
      RHOINI = 1.0E-12,
      DRFUEL = 0.15E-3,
      ROFUEL = 224.0,
      ZFUEL = 39,
      DRPUSH = 0.37E-3,
      ROPUSH = 1.26E3,
      ZPUSH = 35,
      DRTMPR = 0.14E-3,
      ROTMPR = 1.13E4,
      ZTMPR = 15,
      LASER1(21) = 1.97,
      LASER1(22) = 0.5,
      LASER1(23) = 1.5E-8,
      LASER1(24) = 2.1E-8,
      LASER1(25) = 2.4E-8,
      LASER1(26) = 3.1E-8,
      LASER1(27) = 1.9E11,
      LASER1(28) = 2.39E12,
      LASER1(29) = 3.98E13,
```

```
MESH = 90,
NRUN = 10000,
NPRNT = 100,
SAHA = 1.0,
NLPFE = F,
STATE = 3.0,
TINUCL = 5.8E7,
TEINI = 500.0,
TIINI = 500.0,
NLBRMS = F,
&END
```

For the rest of the variables in the Namelist NEWRUN the default values are given in Chapter 4.

5.2 Discussion of Results

We now present a brief summary of the simulation results obtained by one-dimensional implosion of the target shown in Fig. 6 using the set of input parameters given in section 5.1. In Fig. 12 we plot the trajactories of the inner fuel boundary, the pusher fuel boundary, the end of the absorption region, the tamper-pusher boundary and the outer tamper boundary respectively as a function of time. It is seen that the fuel and the payload shell (tamper part of the pusher around the fuel) move inwards by the high pressure in the absorption region behind the payload shell. The effects of the first and the second shocks can also be seen in the fuel region at t $\sim$ 18 ns and 26 ns respectively. Ignition takes place at t $\sim$ 36.33 ns and the entire burn process is finished in 120 ps and the fuel and the payload expand. The tamper-pusher boundary, on the other hand, maintains a steady position during the implosion and the burn until the expanding fuel and pusher material hits the tamper at t $\sim$ 41 ns and the tamper then expands fast.

The overall gain of this target is 179 and it yields an output energy $\sim$ 784 MJ for an input energy $\sim$ 4.38 MJ. Further details of the results are shown in the following table.

Table

Summary of the Results

Prepulse Power P_1 (TW)	:	2.4
Peak Power P_3 (TW)	:	500
Input Energy (MJ)	:	4.38
Output Energy (MJ)	:	784
Gain	:	179
Fractional Burn ϕ (%)	:	56
Fuel ρR at Ignition (g/cm^2)	:	4.3
Tamper ρR at Ignition (g/cm^2)	:	1.82
Time of Ignition (ns)	:	36.33
Burn Time (ps)	:	120

We note that the logical switch NLBRMS was set .False. in these calculations. This is because the treatment of radiation losses in MEDUSA-KA is not very accurate. One needs a proper radiation transport model to simulate the radiation effects. At the time of ignition, the central burning zone is optically thin towards the thermal radiation /13/ while the surrounding cold and dense fuel is optically thick. The thermal radiation from the central burning zone will therefore be absorbed in the surrounding fuel, thereby heating it and spreading the burn. It is therefore an extremely bad approximation to switch on Bremsstrahlung in the MEDUSA-KA code in these pellet calculations.

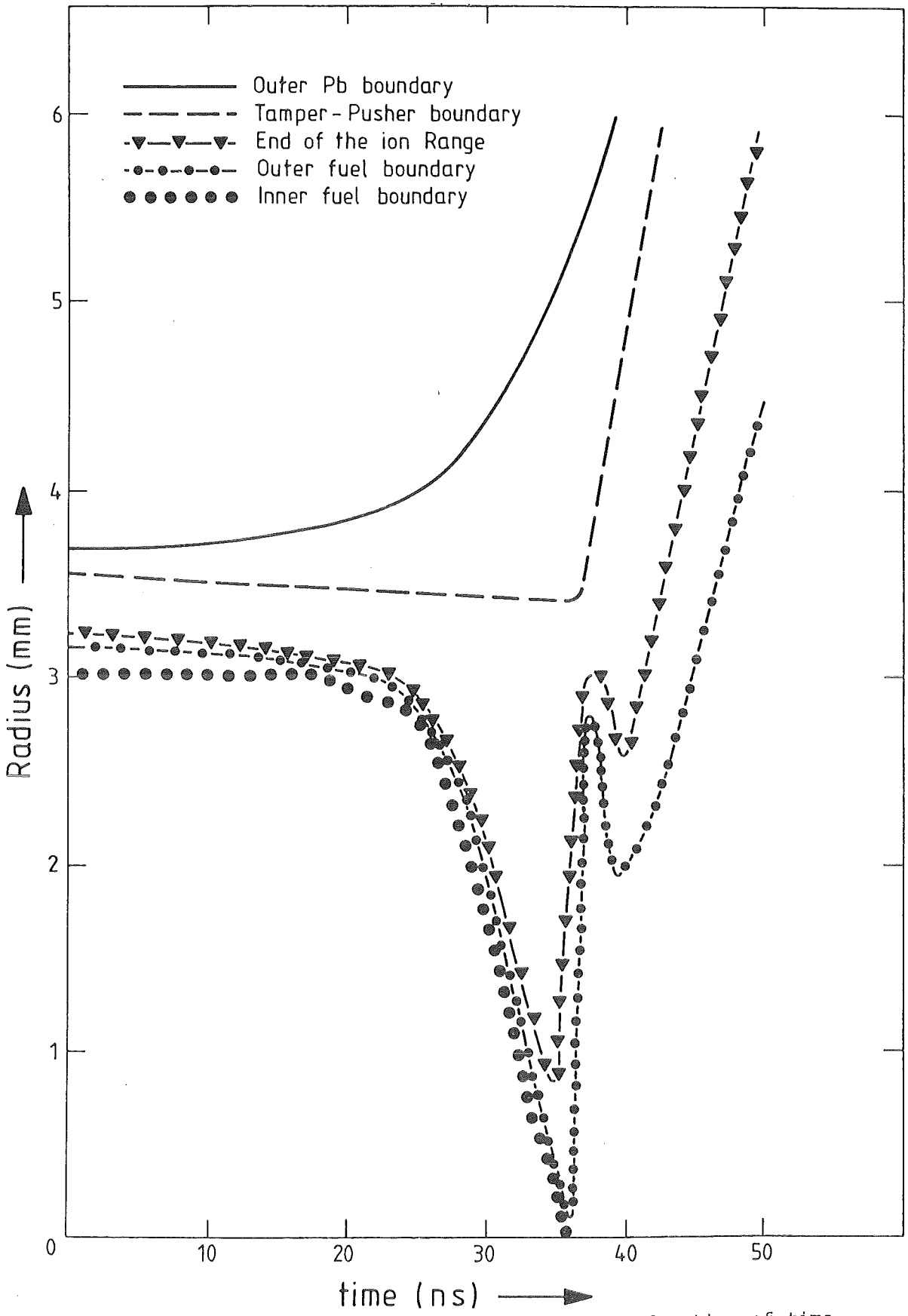

Fig.12: Co-ordinates of material interfaces as a function of time.

5.3 Selected Output from MEDUSA-KA Test Run

The selected output obtained from the updated version of MEDUSA-KA using the input data file described in section 5.1 is presented at four different time levels. These time levels are at t = 0, which represents initial conditions, t = 36.25 ns, a time just before ignition, at t = 36.38 ns, a time when substantial fraction of the fuel is burning and t = 45.14 ns when the target has disassembled. It is seen from the print out that the code only prints those common variables and common arrays which are of importance and direct relevance to the implosion and burn of the target. If required, other variables and arrays can also be printed out by inserting appropriate WRITE statements in the SUBROUTINE MPRINT which is the main printing ROUTINE in MEDUSA-KA.

TIMESTEP NUMBER 0 TIME = 0.0 DELTA T = 1.0000001E-18

BOUNDARY : R = 3.6800E-03 U = 0.0 P = 1.0000E-60 TI = 0.0 TE = 0.0 SOUND SPEED = 1.2146E+02

ENERGIES : THERMAL -7.53843E+01 KINETIC 0.0 NUCLEAR 0.0 ERROR 0.0 RHO R 3.29772E+01

LASER POWER : 1.90000E+11 WATTS TOTAL ENERGY INPUT FROM LASER 0.0 JOULE ABSORPTION AT R = 3.2281E-03

COORDINATES (M) * 1.00000E+00

0.0	3.0238E-03	3.0315E-03	3.0392E-03	3.0469E-03	3.0546E-03	3.0623E-03	3.0700E-03	3.0777E-03	3.0854E-03
3.0931E-03	3.1008E-03	3.1085E-03	3.1162E-03	3.1238E-03	3.1315E-03	3.1392E-03	3.1469E-03	3.1546E-03	3.1623E-03
3.1700E-03	3.1911E-03	3.2123E-03	3.2334E-03	3.2546E-03	3.2757E-03	3.2969E-03	3.3180E-03	3.3391E-03	3.3603E-03
3.3814E-03	3.4026E-03	3.4237E-03	3.4449E-03	3.4660E-03	3.4871E-03	3.5083E-03	3.5294E-03	3.5493E-03	3.5680E-03
3.5867E-03	3.6053E-03	3.6240E-03	3.6427E-03	3.6613E-03					

HYDRODYNAMIC VELOCITIES (M/SEC) * 1.00000E+00

0.0	0.0	0.0	0.0	0.0	0.0	0.0	0.0	0.0	0.0
0.0	0.0	0.0	0.0	0.0	0.0	0.0	0.0	0.0	0.0
0.0	0.0	0.0	0.0	0.0	0.0	0.0	0.0	0.0	0.0
0.0	0.0	0.0	0.0	0.0	0.0	0.0	0.0	0.0	0.0
0.0	0.0	0.0	0.0	0.0					

LOG(DENSITY (KG/M**3) * 1.00000E+00)

-12.00000	2.35025	2.35025	2.35025	2.35025	2.35025	2.35025	2.35025	2.35025	2.35025
2.35025	2.35025	2.35025	2.35025	2.35025	2.35025	2.35025	2.35025	2.35025	2.35025
3.10037	3.10037	3.10037	3.10037	3.10037	3.10037	3.10037	3.10037	3.10037	3.10037
3.10037	3.10037	3.10037	3.10037	3.10037	3.10037	3.10037	3.10037	4.05308	4.05308
4.05308	4.05308	4.05308	4.05308	4.05308					

LOG(HYDRODYNAMIC PRESSURE (JOULE/M**3) * 1.00000E+00)

-5.08210	8.00003	8.00003	8.00003	8.00003	8.00003	8.00003	8.00003	8.00003	8.00003
8.00003	8.00003	8.00003	8.00003	8.00003	8.00003	8.00003	8.00003	8.00003	8.00003
8.00003	8.00003	8.00003	8.00003	8.00003	8.00003	8.00003	8.00003	8.00003	8.00003
8.00003	8.00003	8.00003	8.00003	8.00003	8.00003	8.00003	8.00003	8.00008	8.00008
8.00008	8.00008	8.00008	8.00008	8.00008					

LOG(ION TEMPERATURE (DEGREE K) * 1.00000E+00)

2.69897	2.69897	2.69897	2.69897	2.69897	2.69897	2.69897	2.69897	2.69897	2.69897
2.69897	2.69897	2.69897	2.69897	2.69897	2.69897	2.69897	2.69897	2.69897	2.69897
2.69897	2.69897	2.69897	2.69897	2.69897	2.69897	2.69897	2.69897	2.69897	2.69897
2.69897	2.69897	2.69897	2.69897	2.69897	2.69897	2.69897	2.69897	2.69897	2.69897
2.69897	2.69897	2.69897	2.69897	2.69897					

LOG(ELECTRON TEMPERATURE (DEGREE K) * 1.00000E+00)

2.69897	2.69897	2.69897	2.69897	2.69897	2.69897	2.69897	2.69897	2.69897	2.69897
2.69897	2.69897	2.69897	2.69897	2.69897	2.69897	2.69897	2.69897	2.69897	2.69897
2.69897	2.69897	2.69897	2.69897	2.69897	2.69897	2.69897	2.69897	2.69897	2.69897
2.69897	2.69897	2.69897	2.69897	2.69897	2.69897	2.69897	2.69897	2.69897	2.69897
2.69897	2.69897	2.69897	2.69897	2.69897					

AVERAGE Z

1.00000	1.00000	1.00000	1.00000	1.00000	1.00000	1.00000	1.00000	1.00000	1.00000
1.00000	1.00000	1.00000	1.00000	1.00000	1.00000	1.00000	1.00000	1.00000	1.00000
1.41011	1.41011	1.41011	1.41011	1.41011	1.41011	1.41011	1.41011	1.41011	1.41011
1.41011	1.41011	1.41011	1.41011	1.41011	1.41011	1.41011	1.41011	1.81356	1.81356
1.81356	1.81356	1.81356	1.81356	1.81356					

TIMESTEP NUMBER 5100 TIME = 3.6250288E-08 DELTA T = 8.5865603E-13

DELTA T DETERMINED BY CONDITION 1 AT MESHPOINT 10

BOUNDARY : R = 5.2358E-03 U = 1.6132E+05 P = 1.0000E-60 TI = 0.0 TE = 0.0 SOUND SPEED = 4.1411E+04

ENERGIES : THERMAL 2.78998E+05 KINETIC 6.96780E+04 NUCLEAR 0.0 ERROR -3.47750E+02 RHO R 4.28676E+00

COORDINATES (M) * 1.00000E+00

0.0	6.0233E-05	7.7815E-05	8.5142E-05	8.9061E-05	9.1735E-05	9.4264E-05	9.6630E-05	9.8837E-05	1.0102E-04
1.0309E-04	1.0516E-04	1.0725E-04	1.0935E-04	1.1142E-04	1.1345E-04	1.1545E-04	1.1739E-04	1.1928E-04	1.2105E-04
1.2282E-04	1.6534E-04	8.7401E-04	1.7642E-03	2.1841E-03	2.4175E-03	2.5734E-03	2.6945E-03	2.7954E-03	2.8829E-03
2.9605E-03	3.0311E-03	3.0964E-03	3.1574E-03	3.2144E-03	3.2681E-03	3.3188E-03	3.3673E-03	3.5018E-03	3.6930E-03
3.8598E-03	4.0178E-03	4.1812E-03	4.3596E-03	4.5978E-03					

HYDRODYNAMIC VELOCITIES (M/SEC) * 1.00000E+00

0.0	-2.6227E+04	-2.6481E+04	-2.7831E+04	-8.4890E+04	-1.3653E+05	-1.3236E+05	-8.4478E+04	-9.0123E+04	-7.8095E+04
-6.5896E+04	-5.3145E+04	-3.9703E+04	-3.0883E+04	-2.3412E+04	-1.7362E+04	-1.4754E+04	-1.2254E+04	-1.2700E+04	-1.0961E+04
-1.3706E+04	-2.4941E+05	-9.2234E+04	-7.5345E+04	-5.9451E+04	-4.8988E+04	-4.0258E+04	-3.3596E+04	-2.8302E+04	-2.5019E+04
-2.2154E+04	-1.9326E+04	-1.6436E+04	-1.3271E+04	-1.0351E+04	-7.2244E+03	-4.3178E+03	-1.3620E+03	9.1543E+03	2.6309E+04
4.1543E+04	5.5505E+04	7.1355E+04	8.7341E+04	1.0586E+05					

LOG(DENSITY (KG/M**3) * 1.00000E+00)

5.31423	5.24232	5.40814	5.72226	5.83305	5.85796	5.89724	5.87771	5.87809	5.88473
5.86769	5.85165	5.83546	5.82474	5.81871	5.81324	5.81419	5.81056	5.81949	5.84242
5.70490	4.46473	2.27717	2.20788	2.32758	2.45026	2.52469	2.57783	2.61818	2.65187
2.67821	2.69932	2.71717	2.73518	2.75189	2.76826	2.78295	2.76884	3.02341	3.05201
3.05507	3.01409	2.95444	2.82483	2.52944					

LOG(HYDRODYNAMIC PRESSURE (JOULE/M**3) * 1.00000E+00)

17.17789	16.48831	16.48627	16.48956	16.66734	16.68300	16.70581	16.63158	16.60674	16.59384
16.54854	16.50304	16.45847	16.41966	16.39130	16.36717	16.36003	16.34529	16.33766	16.33527
16.20102	14.42954	13.08125	12.86535	12.78676	12.74439	12.71194	12.68840	12.66612	12.64734
12.62661	12.60485	12.58349	12.56750	12.55359	12.54265	12.53369	12.52438	12.47407	12.42126
12.36361	12.26490	12.15594	11.97072	11.60615					

LOG(ION TEMPERATURE (DEGREE K) * 1.00000E+00)

7.63196	7.41391	7.23205	6.84207	6.90561	6.88817	6.85661	6.78587	6.74952	6.71846
6.68190	6.64260	6.60440	6.56361	6.52918	6.49994	6.48529	6.46754	6.43197	6.36673
6.72819	6.35564	7.20783	7.06226	6.86689	6.70593	6.60267	6.52918	6.46960	6.42000
6.37578	6.33575	6.29937	6.26797	6.23985	6.21486	6.19332	6.19768	6.30900	6.24533
6.19769	6.15176	6.11240	6.06764	6.01109					

LOG(ELECTRON TEMPERATURE (DEGREE K) * 1.00000E+00)

7.63198	7.41392	7.23205	6.84208	6.90578	6.88822	6.85664	6.78589	6.74953	6.71846
6.68190	6.64260	6.60440	6.56362	6.52918	6.49994	6.48529	6.46754	6.43197	6.36673
6.72798	6.35564	7.20739	7.06226	6.86702	6.70598	6.60268	6.52919	6.46960	6.42000
6.37579	6.33575	6.29937	6.26797	6.23985	6.21486	6.19332	6.19769	6.30945	6.24575
6.19797	6.15229	6.11307	6.06861	6.01296					

AVERAGE Z

1.00000	1.00000	1.00000	1.00000	1.00000	1.00000	1.00000	1.00000	1.00000	1.00000
1.00000	1.00000	1.00000	1.00000	1.00000	1.00000	1.00000	1.00000	1.00000	1.00000
5.38593	5.31045	7.00000	7.00000	7.00000	7.00000	7.00000	7.00000	7.00000	7.00000
7.00000	7.00000	7.00000	7.00000	7.00000	7.00000	7.00000	7.00000	23.14255	21.87392
19.86224	18.04970	16.61348	15.05948	14.80051					

TIMESTEP NUMBER 5500 TIME = 3.6380591E-08 DELTA T = 1.8143954E-14

DELTA T DETERMINED BY CONDITION 4 AT MESHPOINT 27

BOUNDARY : R = 5.2562E-03 U = 1.6196E+05 P = 1.0000E-60 TI = 0.0 TE = 0.0 SOUND SPEED = 4.1290E+04

ENERGIES : THERMAL 1.95981E+06 KINETIC 1.89545E+05 NUCLEAR 9.42580E+06 ERROR -1.32462E+05 RHO R 4.54435E+00

FUSION : YIELD 2.67168E+01 NEUTRONS 3.31420E+18 RATE 8.75108E+29 ENERGY 7.49301E+06

COORDINATES (M) * 1.00000E+00

0.0	5.6254E-05	7.2720E-05	8.1792E-05	8.8008E-05	9.2473E-05	9.5926E-05	9.8695E-05	1.0091E-04	1.0265E-04
1.0397E-04	1.0558E-04	1.0757E-04	1.0959E-04	1.1162E-04	1.1356E-04	1.1543E-04	1.1725E-04	1.1902E-04	1.2070E-04
1.2241E-04	1.4844E-04	8.6274E-04	1.7546E-03	2.1764E-03	2.4112E-03	2.5682E-03	2.6901E-03	2.7917E-03	2.8796E-03
2.9576E-03	3.0286E-03	3.0943E-03	3.1556E-03	3.2131E-03	3.2672E-03	3.3182E-03	3.3671E-03	3.5030E-03	3.6964E-03
3.8652E-03	4.0245E-03	4.1898E-03	4.3703E-03	4.6109E-03					

HYDRODYNAMIC VELOCITIES (M/SEC) * 1.00000E+00

0.0	-9.7368E+05	-8.3127E+05	-3.4350E+05	5.8396E+04	4.3438E+05	8.0600E+05	1.1256E+06	1.4873E+06	1.9809E+06
2.1946E+06	8.3403E+05	4.3725E+05	1.6987E+05	5.9979E+03	1.1069E+04	1.6107E+04	2.0258E+04	2.3813E+04	2.6622E+04
2.8605E+04	3.3339E+04	-7.9142E+04	-7.1186E+04	-5.7539E+04	-4.7636E+04	-3.9102E+04	-3.2695E+04	-2.7599E+04	-2.4337E+04
-2.1307E+04	-1.8563E+04	-1.5681E+04	-1.2734E+04	-9.9143E+03	-6.8113E+03	-4.0319E+03	-1.0166E+03	9.4332E+03	2.6531E+04
4.1760E+04	5.5842E+04	7.1673E+04	8.7839E+04	1.0640E+05					

LOG(DENSITY (KG/M**3) * 1.00000E+00)

5.29912	5.31121	5.42643	5.50782	5.60280	5.68599	5.75671	5.83376	5.92224	6.04160
6.02071	5.87254	5.84916	5.83165	5.83223	5.83877	5.84102	5.84052	5.84426	5.85949
5.75589	4.61033	2.28414	2.21006	2.32812	2.44897	2.52326	2.57629	2.61673	2.65061
2.67688	2.69731	2.71492	2.73259	2.74887	2.76543	2.77971	2.76449	3.01804	3.04575
3.05247	3.00754	2.94730	2.81751	2.52096					

LOG(HYDRODYNAMIC PRESSURE (JOULE/M**3) * 1.00000E+00)

18.59789	18.19136	18.27675	18.34422	18.44131	18.52269	18.58575	18.64993	18.72119	18.81926
18.71791	18.29933	18.09142	17.33516	16.41429	16.41043	16.40532	16.39569	16.37927	16.36639
16.29741	14.75445	13.09215	12.86905	12.78821	12.74270	12.70976	12.68593	12.66376	12.64529
12.62442	12.60144	12.57966	12.56308	12.54839	12.53777	12.52810	12.51717	12.46681	12.41276
12.36009	12.25593	12.14616	11.96071	11.59475					

LOG(ION TEMPERATURE (DEGREE K) * 1.00000E+00)

9.16686	9.18629	9.14990	9.13593	9.14223	9.14089	9.13034	9.11242	9.08694	9.05400
8.91947	8.33162	8.00454	7.40262	6.53859	6.51743	6.50336	6.48739	6.44823	6.38291
6.77445	6.52971	7.21173	7.06366	6.86767	6.70542	6.60184	6.52821	6.46864	6.41921
6.37494	6.33443	6.29789	6.26627	6.23784	6.21298	6.19118	6.19508	6.30748	6.24351
6.19746	6.14988	6.11030	6.06549	6.00870					

LOG(ELECTRON TEMPERATURE (DEGREE K) * 1.00000E+00)

8.97634	8.96729	8.95381	8.94376	8.93438	8.92430	8.91270	8.89885	8.88265	8.86482
8.84186	8.77562	8.63062	7.82802	6.53859	6.51743	6.50336	6.48739	6.44823	6.38291
6.77445	6.52708	7.21130	7.06377	6.86793	6.70559	6.60197	6.52832	6.46875	6.41926
6.37498	6.33447	6.29791	6.26629	6.23786	6.21300	6.19119	6.19510	6.30797	6.24400
6.19723	6.15037	6.11097	6.06645	6.01059					

AVERAGE Z

1.00000	1.11508	1.12429	1.13069	1.12337	1.11215	1.09912	1.08550	1.06743	1.04562
1.01936	1.00320	1.00032	1.00000	1.00000	1.00000	1.00000	1.00000	1.00000	1.00000
5.47895	5.84060	7.00000	7.00000	7.00000	7.00000	7.00000	7.00000	7.00000	7.00000
7.00000	7.00000	7.00000	7.00000	7.00000	7.00000	7.00000	7.00000	23.08450	21.79750
19.83232	17.97626	16.53656	14.99858	14.79228					

TIMESTEP NUMBER 8800 TIME = 4.5147555E-08 DELTA T = 1.1115354E-11

DELTA T DETERMINED BY CONDITION 1 AT MESHPOINT 40

BOUNDARY : R = 1.3618E-02 U = 1.4930E+06 P = 1.0000E-60 TI = 0.0 TE = 0.0 SOUND SPEED = 1.2181E+05

ENERGIES : THERMAL 3.01180E+06 KINETIC 8.73774E+06 NUCLEAR 6.32120E+07 ERROR -1.62244E+06 RHO R 3.80484E-01

COORDINATES (M) * 1.00000E+00

0.0	8.8073E-04	1.2694E-03	1.5049E-03	1.6839E-03	1.8323E-03	1.9607E-03	2.0750E-03	2.1787E-03	2.2741E-03
2.3628E-03	2.4460E-03	2.5244E-03	2.5988E-03	2.6696E-03	2.7374E-03	2.8024E-03	2.8650E-03	2.9255E-03	2.9840E-03
3.0407E-03	3.6176E-03	4.0499E-03	4.4029E-03	4.7077E-03	4.9815E-03	5.2311E-03	5.4604E-03	5.6728E-03	5.8704E-03
6.0565E-03	6.2340E-03	6.4033E-03	6.5662E-03	6.7236E-03	6.8755E-03	7.0253E-03	7.1647E-03	7.6558E-03	8.2510E-03
8.7924E-03	9.3649E-03	9.9724E-03	1.0673E-02	1.1574E-02					

HYDRODYNAMIC VELOCITIES (M/SEC) * 1.00000E+00

0.0	8.0430E+04	1.1546E+05	1.3533E+05	1.5001E+05	1.6237E+05	1.7368E+05	1.8426E+05	1.9406E+05	2.0309E+05
2.1139E+05	2.1909E+05	2.2629E+05	2.3309E+05	2.3961E+05	2.4586E+05	2.5189E+05	2.5774E+05	2.6338E+05	2.6888E+05
2.7418E+05	3.3192E+05	3.7908E+05	4.1740E+05	4.4318E+05	4.6359E+05	4.8486E+05	5.0622E+05	5.2733E+05	5.4815E+05
5.6438E+05	5.7935E+05	5.9572E+05	6.0684E+05	6.2339E+05	6.3333E+05	6.4068E+05	6.6319E+05	6.5396E+05	6.6665E+05
6.9940E+05	7.7037E+05	8.5695E+05	9.5792E+05	1.0887E+06					

LOG(DENSITY (KG/M**3) * 1.00000E+00)

1.48496	1.48235	1.48418	1.48550	1.48545	1.48508	1.48458	1.48407	1.48326	1.48250
1.48180	1.48114	1.48053	1.48000	1.47948	1.47893	1.47831	1.47759	1.47692	1.47594
1.61974	1.62920	1.63904	1.64607	1.64483	1.64338	1.64559	1.64892	1.65432	1.65871
1.65936	1.65991	1.66143	1.65905	1.66088	1.65428	1.66094	1.68638	1.83091	1.86424
1.77597	1.70543	1.60221	1.45334	1.15861					

LOG(HYDRODYNAMIC PRESSURE (JOULE/M**3) * 1.00000E+00)

13.39249	12.88277	12.88111	12.87890	12.87690	12.87507	12.87320	12.87128	12.86936	12.86760
12.86603	12.86474	12.86361	12.86267	12.86181	12.86099	12.86014	12.85926	12.85837	12.85741
12.85240	12.83855	12.83310	12.82850	12.81570	12.80232	12.79331	12.78633	12.78260	12.77890
12.77153	12.76396	12.75813	12.74793	12.74313	12.72990	12.73036	12.75511	12.53609	12.34916
12.08037	11.90397	11.73021	11.53943	11.25485					

LOG(ION TEMPERATURE (DEGREE K) * 1.00000E+00)

7.70687	7.69871	7.69457	7.69083	7.68761	7.68468	7.68190	7.67922	7.67670	7.67436
7.67220	7.67023	7.66838	7.66665	7.66502	7.66343	7.66187	7.66036	7.65893	7.65767
7.65222	7.61356	7.59980	7.58968	7.57587	7.56136	7.54948	7.53909	7.53122	7.52438
7.51578	7.50696	7.49998	7.49025	7.48473	7.47515	7.47323	7.49308	7.26772	7.09622
6.94780	6.85965	6.79962	6.75858	6.73135					

LOG(ELECTRON TEMPERATURE (DEGREE K) * 1.00000E+00)

7.67600	7.67176	7.66844	7.66576	7.66335	7.66112	7.65902	7.65704	7.65514	7.65333
7.65158	7.64989	7.64824	7.64663	7.64504	7.64349	7.64196	7.64046	7.63897	7.63749
7.63134	7.61037	7.59491	7.58310	7.57191	7.56039	7.54931	7.53903	7.52976	7.52153
7.51362	7.50563	7.49826	7.49074	7.48398	7.47781	7.47101	7.46727	7.28968	7.11010
6.96753	6.88531	6.83092	6.79882	6.80711					

AVERAGE Z

1.00000	1.44589	1.44467	1.44616	1.44186	1.43642	1.43113	1.42670	1.42131	1.41613
1.41089	1.40518	1.39926	1.39327	1.38723	1.38109	1.37490	1.36856	1.36279	1.35630
7.00000	7.00000	7.00000	7.00000	7.00000	7.00000	7.00000	7.00000	7.00000	7.00000
7.00000	7.00000	7.00000	7.00000	7.00000	7.00000	7.00000	7.00000	64.61864	54.68756
54.00465	46.97646	46.42014	46.12294	46.19760					

Acknowledgements

We would like to thank Dr. R. Fröhlich for useful discussions and for reading this manuscript carefully and making useful suggestions as to the structure of this report. We would also like to thank Mr. W. Höbel, Mr. D. Henderson and Dr. B. Goel for pointing out some corrections. We are also thankful to Mr. N. Moritz for help with technical computing problems. Finally we thank Mrs. G. Bunz for typing this manuscript.

References

/1/ J.P. Christiansen, D.E.T.F. Ashby and K.V. Roberts, MEDUSA - A one-dimensional Laser Fusion Code, Comp. Phys. Comm. 7 (1974) 271

/2/ J. Nuckolls et al., Laser-Compression of Matter to Super-High Densities, Nature 239 (1972) 139

/3/ J.S. Clark et al., Laser Driven Implosion of Spherical DT Targets to Thermonuclear Burn, Phys. Rev. Lett. 30 (1973) 89

/4/ N.A. Tahir, Simulation Studies of Laser-Compression of Matter, Ph.D. Thesis, University of Glasgow (1978)

/5/ N.A. Tahir, Incorporation of Radiation Transport into MEDUSA, Rutherford Laboratory Annual Report, RL-79-036 (1979)

/6/ N.A. Tahir, E.W. Laing and D.J. Nicolas, A Radiative Diffusion Model for Laser-Compression Simulations, Rutherford Laboratory Report, RL-80-048 (1980)

/7/ N.A. Tahir and E.W. Laing, Ionization Effects in Laser-Produced Plasmas, Phys. Lett. 79A (1980) 321

/8/ N.A. Tahir and E.W. Laing, Radiation Effects in Gas-Filled Microballoons, Phys. Lett. 77A (1980) 430

/9/ A.R. Bell, New Equation of State for MEDUSA, Rutherford Laboratory Report, RL-80-091 (1981)

/10/ R.G. Evans and A.R. Bell, Laser-Compression Simulations, Rutherford Laboratory Report, RL-80-085 (1980)

/11/ R.G. Evans, MEDUSA: A 1D Fluid Code for the Simulations of Laser Irradiated Targets, University of British Columbia Report No. 75 (1980)

/12/ B. Badger et al., HIBALL - A Conceptual Heavy Ion-Beam Driven Reactor Study, UWFDM-450 and KfK-3202 (1981)

/13/ N.A. Tahir and K.A. Long, Target Design Studies for a Heavy Ion-Beam Driven Inertial Confinement Fusion Reactor, Atomkernenergie/Kerntechnik, 40 (1982) 157

/14/ K.A. Long and N.A. Tahir, Energy Deposition of Ions in Materials and Numerical Simulations of Compression, Ignition and Burn of Ion Beam Driven Inertial Confinement Fusion Pellets, Kernforschungszentrum Karlsruhe Report, KfK-3232 (1981)

/15/ N.A. Tahir and K.A. Long, Fusion Power from Heavy Ion Beam Imploded Targets, Phys. Lett. 90A (1982)

/16/ N.A. Tahir and K.A. Long, Heavy Ion Beam Inertial Confinement Fusion Pellet Simulations, Jahrestagung Kerntechnik, ISSN 0720-9207 (4 - 6 May 1982) 819

/17/ N.A. Tahir, K.A. Long and R. Fröhlich, HIBALL TARGET DESIGN: Ion-Beam Inertial Confinement Fusion Pellet Calculations, Proceedings of the Symposium on Accelerator Aspects of Heavy Ion Fusion, Darmstadt, GSI-82-8 (1982) 598

/18/ N.A. Tahir and K.A. Long, High Gain Pellet Simulations for a Heavy-Ion Beam Fusion Reactor, GSI Darmstadt Annual Report, GSI-82-6 (1981) 53

/19/ R. Fröhlich, B. Goel, D. Henderson, W. Höbel, K.A. Long and N.A. Tahir, Heavy Ion-Beam Driven Inertial Confinement Fusion Target Studies and Reactor Chamber Neutronic Analysis, to be published in Nuclear Engineering and Design (1982)

/20/ J.D. Rose and M. Clarke, Plasma and Controlled Fusion, John Wiley and Sons Inc. (1961)

/21/ R.E. Kidder, Interaction of intense photon and electron beams with plasmas, Proceedings of International School of Physics "Enrico Fermi", Course XLVIII. Academic Press (1971)

/22/ S. Glasstone and R.H. Lovberg, Controlled Thermonuclear Reactions, D Van Nostrand Company Inc. (1960)

/23/ R.E. Kidder and W.S. Barnes, "WAZER, a one-dimensional two-temperature hydrodynamic code," University of California, Livermore Research Report, UCRL-50583

/24/ J. Magill, TRIP - A Time-Dependent Recombination and Ionization Package, Comp. Phys. Comm. 16 (1978) 129

/25/ E.W. Laing and N.A. Tahir, Applications of MEDUSA and Incorporation of Atomic Physics Codes, Rutherford Laboratory Annual Report, RL-78-039 (1978) 3/49

/26/ R.W.P. McWhirter and T.F. Stratton, Plasma Diagnostic Techniques, Academic Press, New York (1965), Editors R.H. Huddelestone and S.L. Leonard

/27/ N.A. Tahir and E.W. Laing, Radiation Effects in Laser-Compression Simulations, Plasma Physics 22 (1980) 1113

/28/ N.A. Tahir, E.W. Laing and D.J. Nicolas, A Multi-Group Treatment of Radiation Transport, Rutherford Laboratory Report, RL-80-083 (1980)

/29/ D. Kershaw, The Incomplete Choleskey-Conjugate Gradient Method for the Iterative Solution of Systems of Linear Equations, J. Comp. Phys. 26 (1978) 43

/30/ Y.B. Zeldovich and Y.P. Raizer, Physics of Shock Waves and High-Temperature Hydrodynamic Phenomenon, Vol. I, Academic Press, New York (1966)

/31/ R.G. Evans, Private Communication

/32/ R. Latter, Temperature Behaviour of the Thomas-Fermi Statistical Model for Atoms, Phys. Rev. 99 (1955) 1854

/33/ N.H. March, Thomas-Fermi Approximation in Quantum Mechanics, Adv. Phys. 6 (1955) 1

/34/ D.A. Kirzhnits, The Limits of Applicability of the Quantum-Classical Equation of State of Matter, Sov. Phy. JETP8 (1959) 1081

/35/ B.I. Bennett, J.D. Johnson, G.I. Kerley and G.T. Rood, An Invitation to the Los Alamos Equation of State Library, Los Alamos Laboratory Report, LA 7130 (1978)

/36/ Wm.H. Read, "TIMEX: A Time-Dependent Explicit Discrete Ordinates Program for the Solution of Multi-Group Transport Equations," Los Alamos Report LA-4800 (July 1972)

/37/ K.A. Long and N.A. Tahir, Heavy Ion Beam ICF Fusion: The Thermodynamics of Ignition and the Achievement of High Gain in ICF Targets, Phys. Lett. 91A (1982) 45

/38/ B. Goel and D.L. Henderson, Neutron Fuel Interaction in HIBALL Target, Symposium on Accelerator Aspects of Heavy Ion Fusion, GSI Darmstadt, March 29 - April 2 (1982) GSI-82-8, 626

/39/ W. Höbel, Private communication